BRACHISTOCHRONES FOR REPULSIVE INVERSE SQUARE FORCE

Garry J. Tee

Department of Mathematics, University of Auckland

Auckland, New Zealand

Abstract

Brachistochrones for inverse square repulsion are expressed in terms of elliptic integrals, as for inverse square attraction. But, the set of brachistochrones is much more complicated than for inverse square attraction. Each pair of points is connected by infinitely many brachistochrones, on each of which the passage time is a local minimum, and the global minimum passage time is attained on one (or on infinitely many) of those curves. The bounded brachistochrones starting at a fixed point are separated from the unbounded brachistochrones by a Critical Brachistochrone, which is expressed in terms of elementary functions.

AMS subject classification: primary 70D05, 49J15 ; secondary 01A45 49-03 70-03

1 Formulæ for Brachistochrones

Under any force field, the path of quickest descent from one point to another is called the brachistochrone for those points. Brachistochrones for central forces have been constructed (Tee, 1999) as the orbits of associated free particles under transformed central forces. The family of brachistochrones starting at a fixed point A (whose polar coordinates are taken as $r = 1,\ \vartheta = 0$) can be parametrized by the angular momentum K of the associated free particle. Here, it is more convenient to parametrize them by $J = 2K^2$.

For inverse square repulsion, at radius $r \geq 1$ the constrained particle has (cf. Tee, 1999, (44)) the speed $v(r)$, where

$$v(r)^2 \ = \ \frac{2(r-1)}{r}, \tag{1}$$

and so $v(r) \nearrow \sqrt{2}$ as $r \nearrow \infty$.

Equations (50), (51) and (52) in (Tee, 1999) then give angle ϑ, arclength s and time t, each as an elliptic integral of radius r, with $r \geq 1$. Thus r is an elliptic function of ϑ, an elliptic function of s, and also an elliptic function of t.

$$\vartheta \;=\; \int_1^r \frac{\mathrm{d}x}{\pm x\sqrt{\frac{x^3}{J(x-1)}-1}}$$
$$\;=\; \int_1^r \frac{(x-1)\sqrt{J}}{\pm x\sqrt{(x-1)\,(x^3-Jx+J)}}\,\mathrm{d}x\;. \tag{2}$$

$$s \;=\; \int_1^r \frac{\mathrm{d}x}{\pm\sqrt{1-\frac{J(x-1)}{x^3}}} \;=\; \int_1^r \frac{x^2}{\pm\sqrt{x(x^3-Jx+J)}}\,\mathrm{d}x\;. \tag{3}$$

$$t \;=\; \int_1^r \frac{\mathrm{d}x}{\mp\sqrt{\frac{2(x-1)}{x}\left(1-\frac{J(x-1)}{x^3}\right)}}$$
$$\;=\; \int_1^r \frac{x^2}{\pm\sqrt{2(x-1)(x^3-Jx+J)}}\,\mathrm{d}x\;. \tag{4}$$

In each of these integrals, the positive square root is to be taken where radius increases with t, and the negative square root is to be taken where radius decreases with t.

The *total angle* of a particle on a brachistochrone is defined as $\int \mathrm{d}\vartheta$. If the particle has wound more than once around the centre, then the total angle is greater than 2π.

The integrands (2), (3) and (4) each contain the cubic polynomial

$$c(x) \;\stackrel{\text{def}}{=}\; x^3 - Jx + J. \tag{5}$$

The orbit of the associated free particle with angular momentum K has an apsidal radius R, if and only if $K = R/v(R)$ (cf. Tee, 1999, (25)). In terms of $J = 2K^2$,

$$J \;=\; \frac{2R^2}{v(R)^2} \;=\; \frac{R^3}{R-1}, \tag{6}$$

in view of (1), and so

$$\frac{\mathrm{d}J}{\mathrm{d}R} \;=\; 2\left(\frac{R}{R-1}\right)^2\left(R-\tfrac{3}{2}\right). \tag{7}$$

Hence for real $R > 1$, J attains its minimum value $J = \frac{27}{4}$ at $R = \frac{3}{2}$.

Therefore, orbits with $J < \frac{27}{4}$ do not have any apse — e.g. with $J = 0$ the constrained particle accelerates radially outwards, with speed $v(r) \nearrow \sqrt{2}$ as r increases (cf. Tee, 1999, (48)).

2 Bounded Brachistochrones

If the brachistochrone has an apsidal radius $r = R$, then

$$0 \;=\; \frac{\mathrm{d}r}{\mathrm{d}\vartheta} \;=\; \frac{\mathrm{d}r}{\mathrm{d}s} \;=\; \frac{\mathrm{d}r}{\mathrm{d}t} \tag{8}$$

at the apse. The integrands in (2), (3) & (4) are $\mathrm{d}\vartheta/\mathrm{d}r$, $\mathrm{d}s/\mathrm{d}r$ & $\mathrm{d}t/\mathrm{d}r$ respectively; and thus with $x = R$ the denominator of each integrand is zero. Hence, the cubic polynomial $c(x)$ must have $x - R$ as a factor.

Therefore, each of the integrands in (2), (3) & (4) has an integrable singularity at the apse.

For fixed J, equation (6) gives an equation in R:

$$R^3 - JR + J \;=\; 0, \tag{9}$$

and so R is a zero of the cubic polynomial $c(x)$ in (5).

With $J = \frac{27}{4}$, the osculation of the graphs of $y = x^3$ and $y = J(x-1)$ gives the double root $x = \frac{3}{2}$, with

$$c(x) \;=\; x^3 - Jx + J \;=\; x^3 - \tfrac{27}{4}x + \tfrac{27}{4} \;=\; (x+3)\left(\tfrac{3}{2} - x\right)^2. \tag{10}$$

With $0 < J < \frac{27}{4}$ there is one real root $-3 < x < 0$. With $J > \frac{27}{4}$, this cubic equation (9) in R has 3 real roots (α, β, γ), with $\gamma < -3 < 1 < \alpha < \frac{3}{2} < \beta$. The negative roots have no physical significance, since $R \geq 1$. As J increases from $\frac{27}{4}$ then α decreases and β increases, with $\alpha - 1 = \alpha^3/J \sim 1/J$ and $\beta = \sqrt{J(1-1/\beta)} \sim \sqrt{J}$ as $J \nearrow \infty$. As $J \searrow \frac{27}{4}$ then α increases and β decreases, both to $\frac{3}{2}$. That may conveniently be written as $\alpha \nearrow \frac{3}{2} \swarrow \beta$.

When a particle with $J > \frac{27}{4}$, starting from rest at $r = 1$, reaches the apsidal radius $r = \alpha < \frac{3}{2}$, then it must return to $r = 1$ without reaching any radius $r > \alpha$; since each brachistochrone under central force is symmetric about each apsidal line (Tee, 1999, §2.1). Hence, the root $\beta > \frac{3}{2}$ of the cubic equation (6) cannot be the radius of any point on that brachistochrone, with $J > \frac{27}{4}$. Therefore, the only apsidal radius is the smaller positive root $R = \alpha < \frac{3}{2}$.

Hence the brachistochrone has an apsidal radius R if and only if $J > \frac{27}{4} = 6{\cdot}75$; and $1 < R < \frac{3}{2}$. We call this a *bounded brachistochrone*, and it can be parametrized by the maximum radius R, as an alternative to J. Applying Vieta's method for solving the cubic equation (9) with 3 real roots, we get the explicit expression:

$$R \;=\; \sqrt{\frac{4J}{3}}\;\sin\left(\frac{1}{3}\arcsin\sqrt{\frac{27}{4J}}\right)\;. \tag{11}$$

As $J \nearrow \infty$ then $R - 1 \sim 1/J$, and so the bounded brachistochrone approaches the form of a cycloid, generated by a circle of diameter $1/J$.

Since R is a root of the cubic equation (9), the cubic polynomial $c(x)$ has the factor $x - R$:

$$\begin{aligned} c(x) \;&=\; x^3 - Jx + J \;=\; x^3 - \frac{R^3}{R-1}\,x + \frac{R^3}{R-1} \\ &\equiv\; (x-R)\left(x^2 + Rx - \frac{R^2}{R-1}\right)\;. \end{aligned} \tag{12}$$

Define the quadratic polynomial $q(x) \stackrel{\text{def}}{=} x^2 + Rx - R^2/(R-1)$, so that $q(x) > 0$ for all sufficiently large $|x|$. Then, $q(1) = 1/(1-R) < 0$, so that q has one real zero less than 1; and $q(R) = (2R-3)R^2/(R-1) < 0$, since $R < \frac{3}{2}$, so that the other zero of q is greater than R. Therefore, the quadratic polynomial $q(x) < 0$, for all $x \in [1, R]$.

On the first half–arch of the brachistochrone, r is an increasing function of t. The equations (2), (3) and (4) (cf. Tee, 1999, (55), (56), (57)) give angle, arclength and

time on the first half–arch; each as an elliptic integral of radius with the maximum radius R as a parameter:

$$\begin{aligned}\Theta(r,R) &= \int_1^r \frac{x-1}{x\sqrt{(x-1)\left(\left(\frac{R-1}{R^3}\right)x^3+x-1\right)}}\,\mathrm{d}x \\ &= \sqrt{\tfrac{R^3}{R-1}}\int_1^r \frac{x-1}{x\sqrt{(x-1)(R-x)\left[-x^2-Rx+\frac{R^2}{R-1}\right]}}\,\mathrm{d}x\ . \end{aligned} \tag{13}$$

$$\begin{aligned}S(r,R) &= \int_1^r \frac{x^2}{\sqrt{x\left(x^3+\left(\frac{R^3}{R-1}\right)(x-1)\right)}}\,\mathrm{d}x \\ &= \int_1^r \frac{x^2}{\sqrt{x(R-x)\left[-x^2-Rx+\frac{R^2}{R-1}\right]}}\,\mathrm{d}x\ . \end{aligned} \tag{14}$$

$$\begin{aligned}T(r,R) &= \int_1^r \frac{x^2}{\sqrt{2(x-1)\left(x^3+\left(\frac{R^3}{R-1}\right)x-\frac{R^3}{R-1}\right)}}\,\mathrm{d}x \\ &= \int_1^r \frac{x^2}{\sqrt{2(x-1)(R-x)\left[-x^2-Rx+\frac{R^2}{R-1}\right]}}\,\mathrm{d}x\ . \end{aligned} \tag{15}$$

In these 6 integrands, every factor is strictly positive for all $x \in (1,R)$.

Each brachistochrone is symmetric about each apsidal line; and hence on the second half–arch the negative square roots are taken in (2), (3) and (4), giving

$$\vartheta = 2\Theta(R,R)-\Theta(r,R),\ s = 2S(R,R)-S(r,R),\ t = 2T(R,R)-T(r,R). \tag{16}$$

Or (cf. Tee, 1999, (58)), if angle ω, arclength σ and time τ are measured from the apse, then the complete brachistochrone is given in terms of r by the elliptic integrals

$$\begin{aligned}\omega &= \pm\sqrt{\tfrac{R^3}{R-1}}\int_r^R \frac{x-1}{x\sqrt{(x-1)(R-x)\left[-x^2-Rx+\frac{R^2}{R-1}\right]}}\,\mathrm{d}x\ , \\ \sigma &= \pm\int_r^R \frac{x^2}{\sqrt{x(R-x)\left[-x^2-Rx+\frac{R^2}{R-1}\right]}}\,\mathrm{d}x\ , \\ \tau &= \pm\int_r^R \frac{x^2}{\sqrt{2(x-1)(R-x)\left[-x^2-Rx+\frac{R^2}{R-1}\right]}}\,\mathrm{d}x\ . \end{aligned} \tag{17}$$

2.1 Angle as a Function of Radius for Bounded Brachistochrones

The elliptic integral (13) has a singularity in the derivative of the integrand at $x=1$, and when $r=R$ it has an integrable singularity at $x=R$. Those singularities may

be eliminated by an appropriate change of variable, to produce a smooth integrand which is suitable for quadrature by Romberg integration.

2.1.1 Elimination of Singularities

In (13), substitute

$$x \;=\; x(\zeta) \;= \tfrac{1}{2}(1 + R + (1 - R)\cos\,\zeta), \tag{18}$$

so that as x increases from 1 to $R < \frac{3}{2}$, ζ increases from 0 to π, and

$$\zeta \;= \zeta(x) \;=\; \arccos\left(\frac{2x - 1 - R}{1 - R}\right), \tag{19}$$

with

$$\frac{\mathrm{d}x}{\sqrt{(x-1)(R-x)}} \;=\; \mathrm{d}\zeta, \tag{20}$$

as in (Tee, 1999, (79) & (80)). Then, the integral (13) becomes

$$\Theta(r, R) \;=\; \int_0^{\zeta(r)} \frac{x-1}{x}\sqrt{\frac{R^3}{R^2 - (R-1)x(x+R)}}\;\mathrm{d}\zeta\;, \tag{21}$$

where the function $x(\zeta)$ is given by (18). In particular, the apse angle is

$$\Theta(R, R) \;=\; \int_0^{\pi} \frac{x-1}{x}\sqrt{\frac{R^3}{R^2 - (R-1)x(x+R)}}\;\mathrm{d}\zeta\;. \tag{22}$$

And these transformed integrals are suitable for Romberg integration with respect to ζ.

Apsidal Locus The curve $\vartheta = \Theta(R, R)$, which we shall call the *apsidal locus*, separates those points C for which the brachistochrone AC is part of the (open) first half–arch (13) of a complete bounded brachistochrone AB, from those points C for which the brachistochrone AC includes part of the (open) second half–arch (16).

2.1.2 Pictures of Bounded Brachistochrones

Each bounded brachistochrone is symmetric about its apsidal radius.

Figure 1 shews the complete brachistochrones for $R = 1{\cdot}05\ (0{\cdot}05)\ 1{\cdot}45$, with the total angle for each complete brachistochrone here being less than π. Note that the small brachistochrones do indeed resemble cycloids, as expected. Also, there is shewn the limit of those curves as $R \nearrow \frac{3}{2}$ (and $(J \searrow \frac{27}{4})$, which is the Critical Brachistochrone with $J = \frac{27}{4}$ (cf. Figure 11). That limit is not symmetric.

Figure 2 shews the first and fifth quadrants of the Critical Brachistochrone and of the apsidal locus, which is computed from (22). All first half–arches of bounded brachistochrones are confined between the apsidal locus and the Critical Brachistochrone.

Figure 1. Bounded Brachistochrones, for maximum radius R = 1.05 (0.05) 1.45

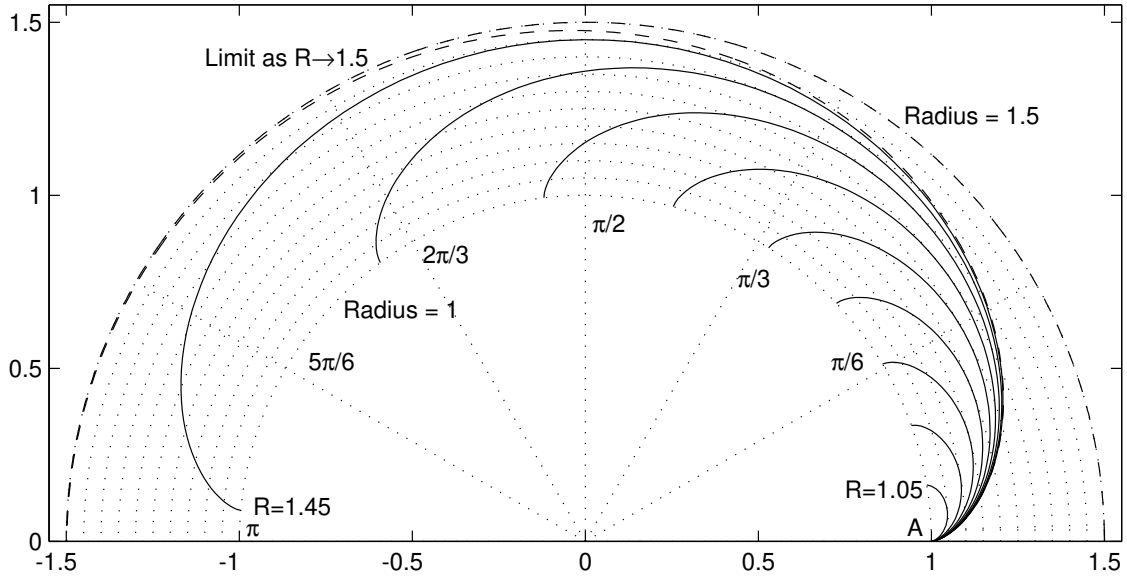

Figure 2. Apsidal Locus and Critical Brachistochrone, 1st and 5th Quadrant

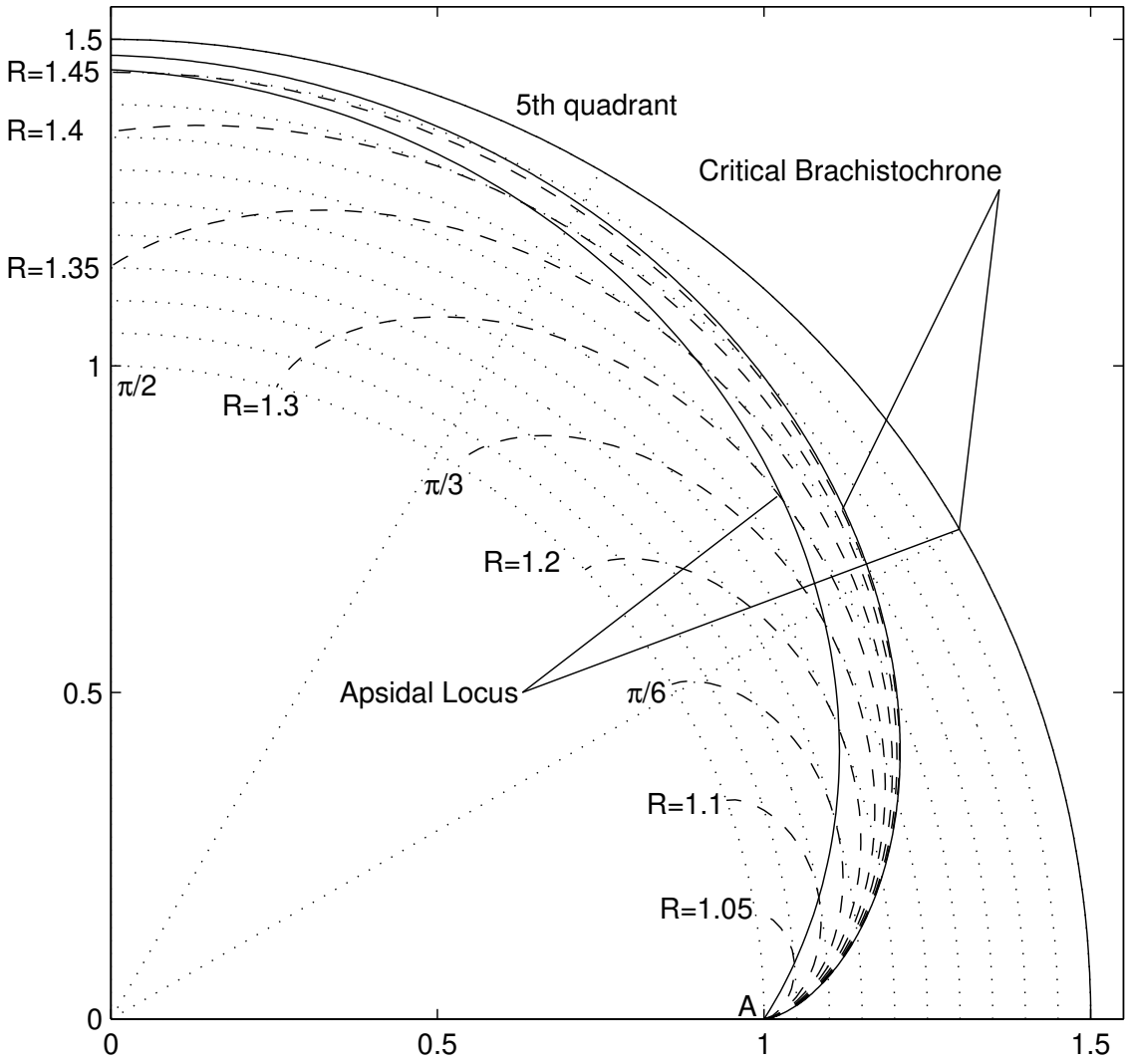

Both the apsidal locus and the Critical Brachistichrone have unbounded total angle ϑ, each spiralling out asymptotically towards the critical radius $r = \frac{3}{2}$, without reaching it. After winding once around O, in the 5th quadrant both the apsidal locus and the Critical Brachistochrone are very close to the critical radius $r = \frac{3}{2}$.

Figure 3 shews the complete brachistochrones for $R = 1{\cdot}45\ (0{\cdot}0025)\ 1{\cdot}4975$, with the total angle for complete brachistochrone ranging from slightly less than π to slightly more than 2π, after winding once around O.

The curve with $R = 1{\cdot}495$ and total angle Γ (where Γ is close to $\frac{11}{6}\pi$), is the unique complete brachistochrone with total angle of Γ. But the least time for the particle to get from A to that point is given by the complete brachistochrone with total angle $2\pi - \Gamma$, which is close to $\frac{1}{6}\pi$. The curve with $R = 1{\cdot}4975$ and total angle $\Delta = 6{\cdot}558156305167508$ is the unique complete brachistochrone with total angle of Δ. But the least time for the particle to get from A to that point is given by the complete brachistochrone with total angle $\Delta - 2\pi = 0{\cdot}274970997987922$. And similarly for all brachistochrones with total angle greater than π.

Note that the complete brachistochrone with $R = 1{\cdot}4975$ intersects itself, at $\vartheta = 0{\cdot}137485498993961 \equiv 2\pi + 0{\cdot}137485498993961 \pmod{2\pi}$.

Figure 3. Bounded Brachistochrones, for maximum radius R = 1.45 (0.0025) 1.4975

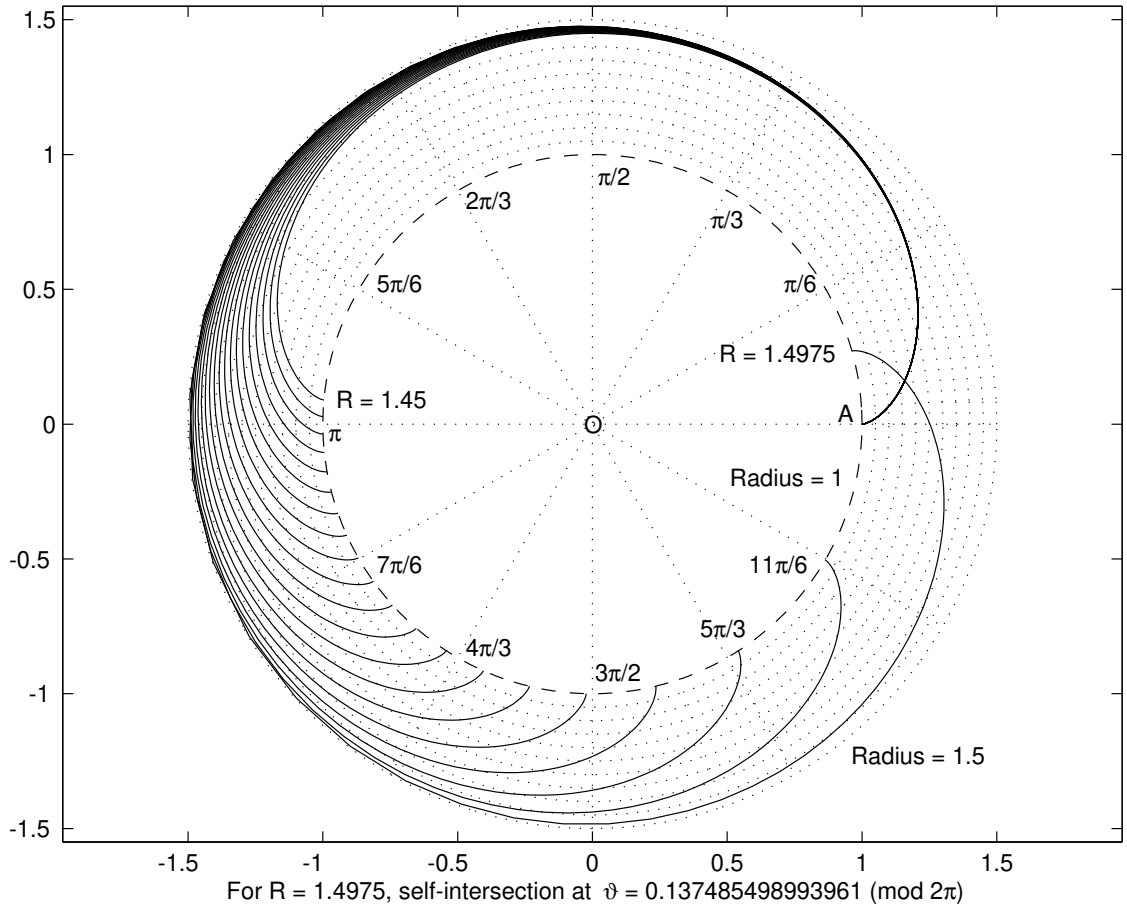

Figure 4 shews the complete brachistochrones (computed similarly to Table 1 in (Tee, 1999)) for $R = 1{\cdot}45358367584520$ with total angle π from A to D; and for $R = \tilde{R} = 1{\cdot}49682968195505$, winding once around O with total angle 2π from A to A. Hence, at $\vartheta = \frac{1}{2}\pi$, the apsidal locus (Figure 2) has radius $1{\cdot}45358367584520$.

The curve with total angle π could be rotated through any angle about the line OA, producing infinitely many complete brachistochrones connecting the diametrically opposite points A and D; and similarly for brachistochrones with total angle which is any integer multiple of π. The curve of least time with total angle 2π is the complete brachistochrone with angle of 2π, and it is unique apart from being rotated through any angle around OA. But the least time for the particle to get from A to A is zero, which is achieved by the particle on the complete brachistochrone consisting of the single point A, with zero total angle.

Figure 4. Bounded Brachistochrones with Total Anglesπ and 2π

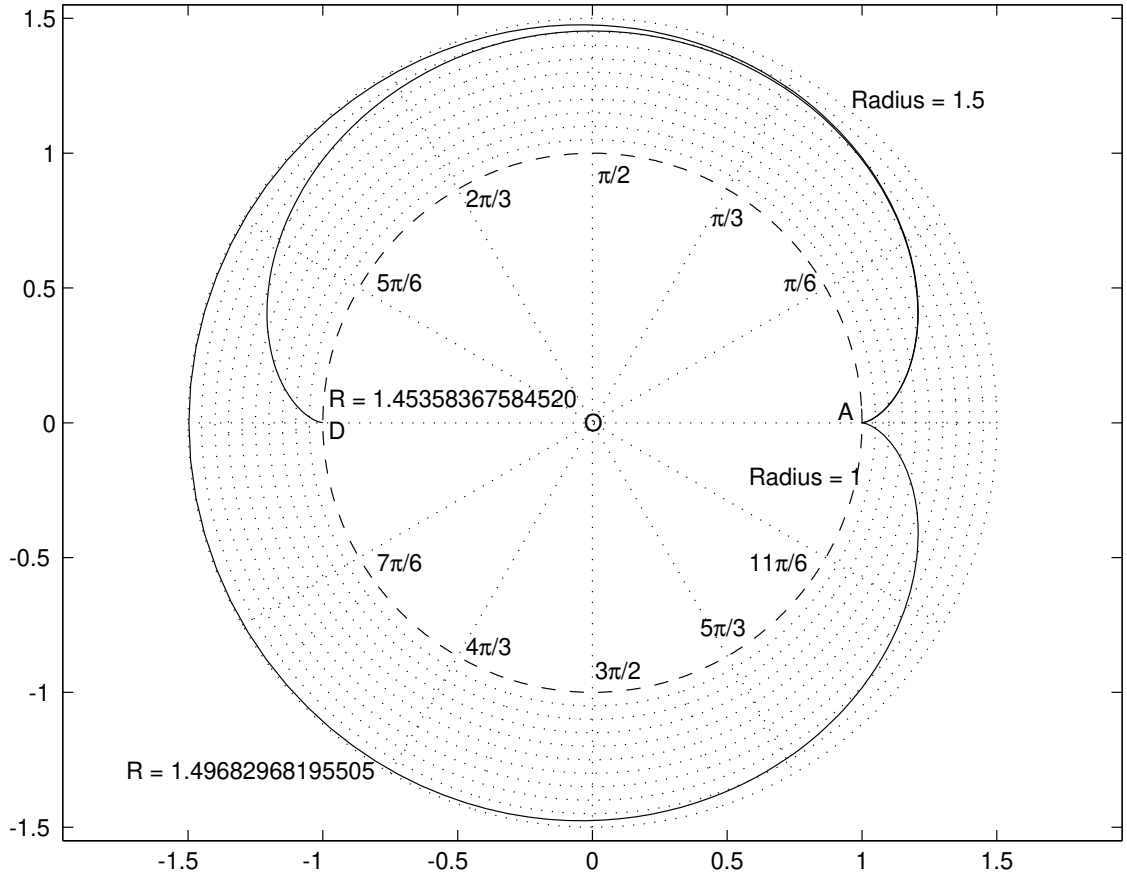

Figure 5 shews the complete brachistochrone for $R = 1{\cdot}49999$, with total angle $\Phi = 12{\cdot}936334846510490$, after winding twice around O. That is the unique curve of least time with total angle of Φ. But the least time for the particle to get from A to that point is given by the complete brachistochrone with total angle $\Phi - 4\pi = 0{\cdot}369964232151317$.

Note that the complete brachistochrone with $R = 1{\cdot}49999$ twice intersects itself, at $\vartheta = 0{\cdot}184982116075658 \equiv 4\pi + 0{\cdot}184982116075658$ and also at $\vartheta = \pi + 0{\cdot}184982116075658 \equiv 3\pi + 0{\cdot}184982116075658$.

2.2 Arclength as a Function of Radius for Bounded Brachistochrones

When $r = R$, the elliptic integral (14) has an integrable singularity at $x = R$. That

singularity may be eliminated by an appropriate change of variable, to produce a smooth integrand which is suitable for quadrature by Romberg integration.

Figure 5. Bounded Brachistochrone, for maximum radius R = 1.49999

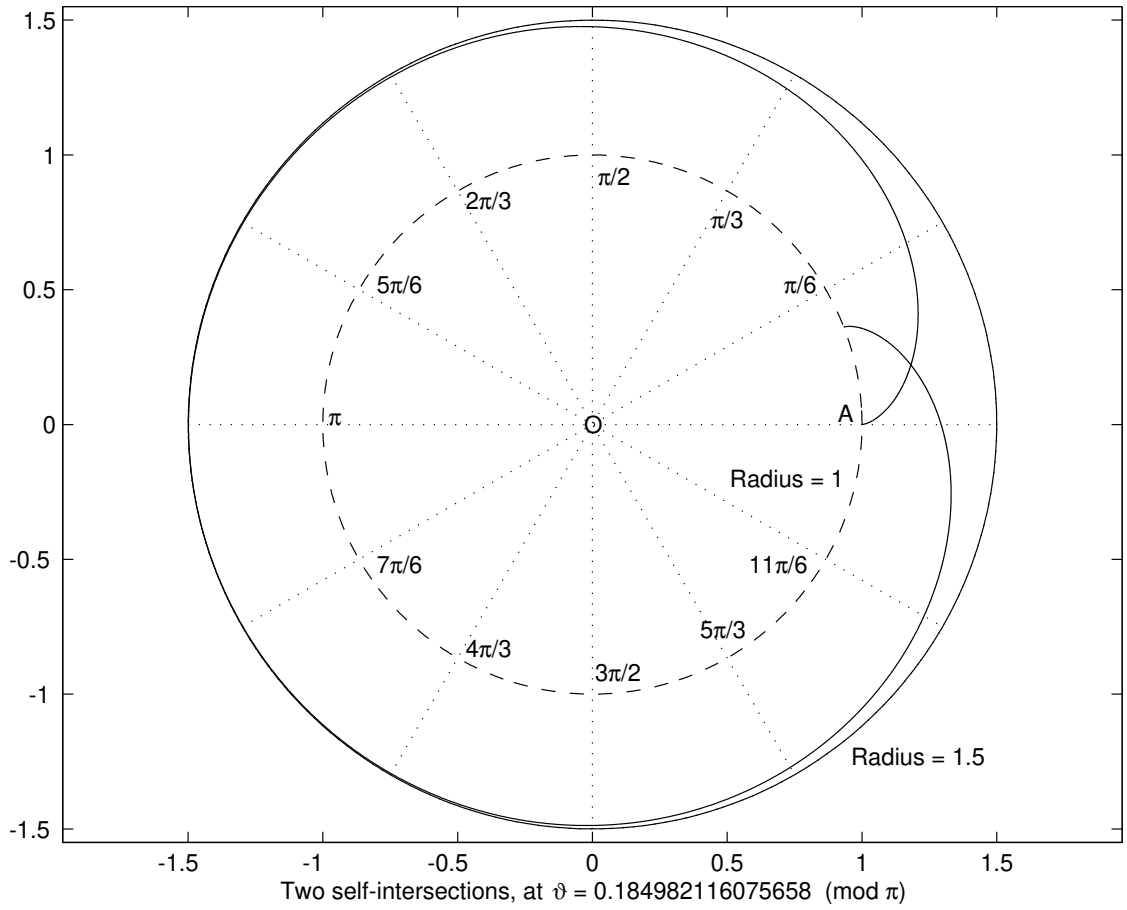

2.2.1 Elimination of Singularity

In the integral (14) for s, substitute

$$x = x(y) = R - y^2, \tag{23}$$

so that $y = \sqrt{R-x}$ and $\mathrm{d}x = -2y\ \mathrm{d}y$ (cf. Tee, 1999, (76)). Hence

$$\begin{aligned} S(r,R) &= \int_{\sqrt{R-r}}^{\sqrt{R-1}} \frac{2yx^2}{y\sqrt{x\left[\frac{R^2}{R-1} - Rx - x^2\right]}}\ \mathrm{d}y \\ &= \int_{\sqrt{R-r}}^{\sqrt{R-1}} \frac{2x}{\sqrt{\frac{R^2}{(R-1)x} - R - x}}\ \mathrm{d}y\ , \end{aligned} \tag{24}$$

where $x = R - y^2$. In particular, the arclength to the apse is

$$S(R,R) = \int_0^{\sqrt{R-1}} \frac{2x}{\sqrt{\frac{R^2}{(R-1)x} - R - x}}\ \mathrm{d}y\ . \tag{25}$$

And these transformed integrals are suitable for Romberg integration with respect to y.

2.2.2 Graphs of Radius versus Arclength

Figure 6 shews graphs of radius versus arclength for $R = 1{\cdot}05\ (0{\cdot}05)\ 1{\cdot}45$, with the radius everywhere less than $1{\cdot}5$. Each graph is symmetric about the line $s = S(R, R)$, for the apse.

Figure 6: Radius versus Arclength, for maximum radius R = 1.05 (0.05) 1.45

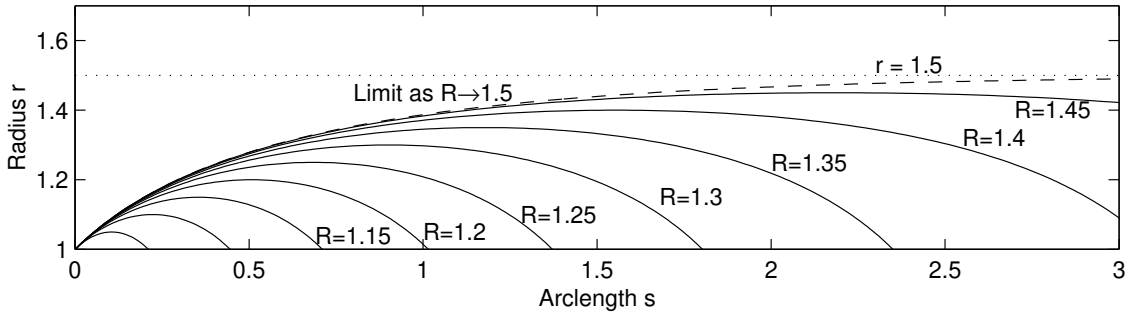

Also, there is shewn the limit of those graphs as $R \nearrow \frac{3}{2}$ (and $J \searrow \frac{27}{4}$), which is the graph for the brachistochrone with $J = \frac{27}{4}$ (cf. §3). That limit is not symmetric.

2.3 Time as a Function of Radius for Bounded Brachistochrones

The elliptic integral (15) has an integrable singularity at $x = 1$, and when $r = R$ it has another integrable sigularity at $x = R$. Those singularities may be eliminated by an appropriate change of variable, to produce a smooth integrand which is suitable for quadrature by Romberg integration.

2.3.1 Elimination of Singularities

With the substitution (18), the integral (15) becomes

$$T(r, R) \;=\; \frac{1}{\sqrt{2}} \int_0^{\zeta(r)} \frac{x^2}{\sqrt{\frac{R^2}{R-1} - x(x+R)}}\, \mathrm{d}\zeta \ , \tag{26}$$

where the function $x(\zeta)$ is given by (18). In particular, the time at the apse is

$$T(R, R) \;=\; \frac{1}{\sqrt{2}} \int_0^{\pi} \frac{x^2}{\sqrt{\frac{R^2}{R-1} - x(x+R)}}\, \mathrm{d}\zeta \ . \tag{27}$$

And these transformed integrals are suitable for Romberg integration with respect to ζ.

2.3.2 Graphs of Radius versus Time

Figure 7 shews graphs of radius versus time for $R = 1{\cdot}05\ (0{\cdot}5)\ 1{\cdot}45$, with the radius everywhere less than $1{\cdot}5$. Each graph is symmetric about the line $t = T(R, R)$, for the apse.

Figure 7: Radius versus Time, for maximum radius R = 1.05 (0.05) 1.45

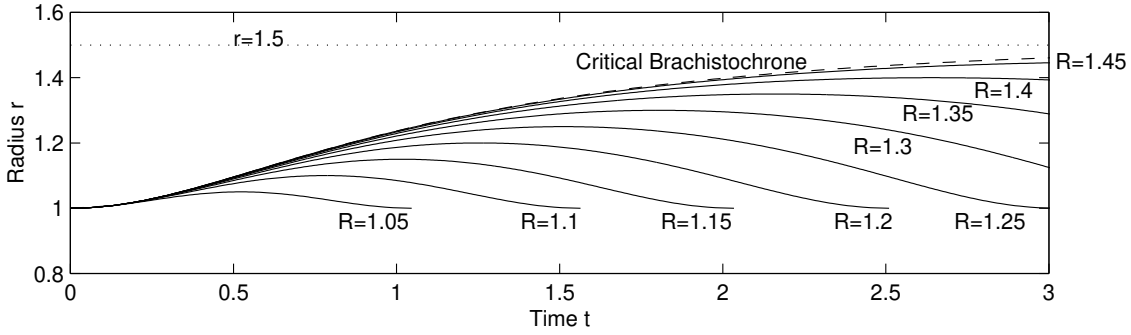

Also, there is shewn the limit of those graphs as $R \nearrow \frac{3}{2}$ (and $J \searrow \frac{27}{4}$), which is the graph for the brachistochrone with $J = \frac{27}{4}$ (cf. §3). That limit is not symmetric.

2.4 Angle, Arclength and Time for Bounded Brachistochrones

Each of ϑ, s and t is a computable function of r. Accordingly, for various values of R, each of the three relations between pairs of these variables can be represented by a graph, with r as the parameter for computing values of the chosen pair of variables. Since each of angle, arclength and time, measured from the apse, is an even function of r, each of these graphs (for each R) is symmetric about its midpoint, corresponding to the apse.

Figure 8: Angle versus Arclength, for maximum radius R = 1.05 (0.05) 1.45

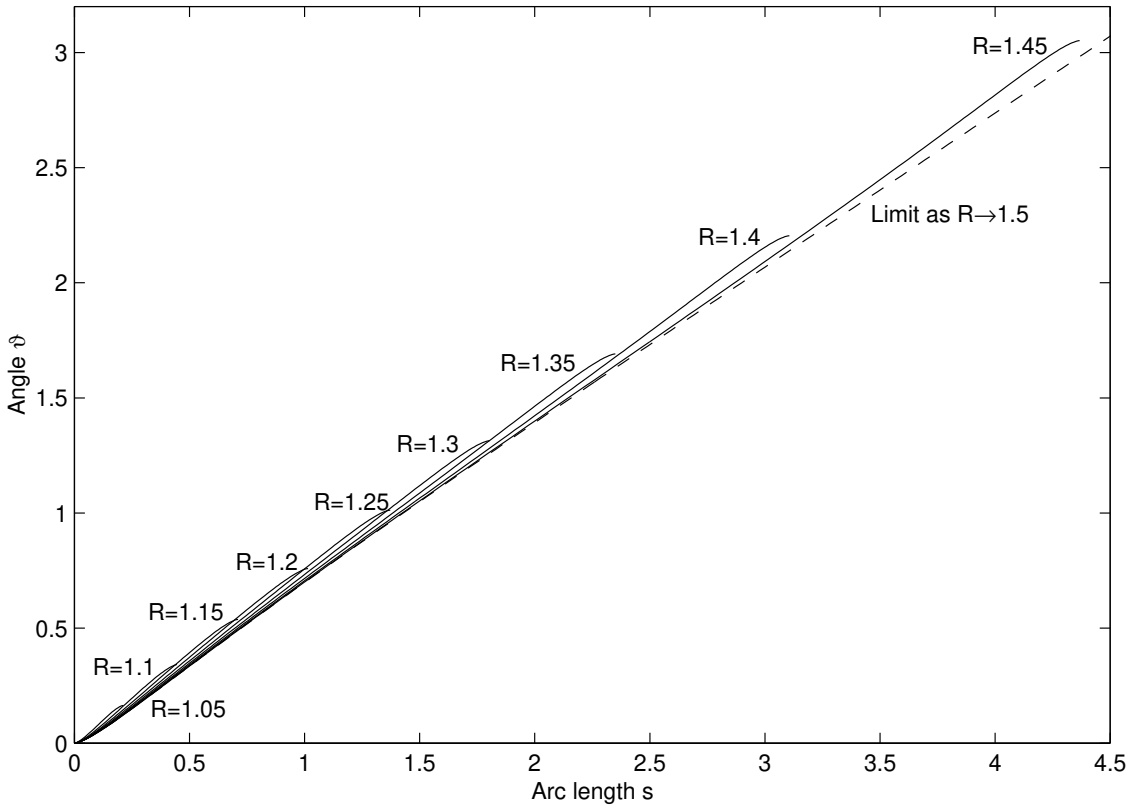

Figure 8 shews graphs of ϑ versus s, Figure 9 shews graphs of ϑ versus t, and Figure 10 shews graphs of s versus t; each for $R = 1{\cdot}05\ (0{\cdot}5)\ 1{\cdot}45$, with the radius everywhere less than $1{\cdot}5$.

Figure 9: Angle versus Time, for maximum radius R = 1.05 (0.05) 1.45

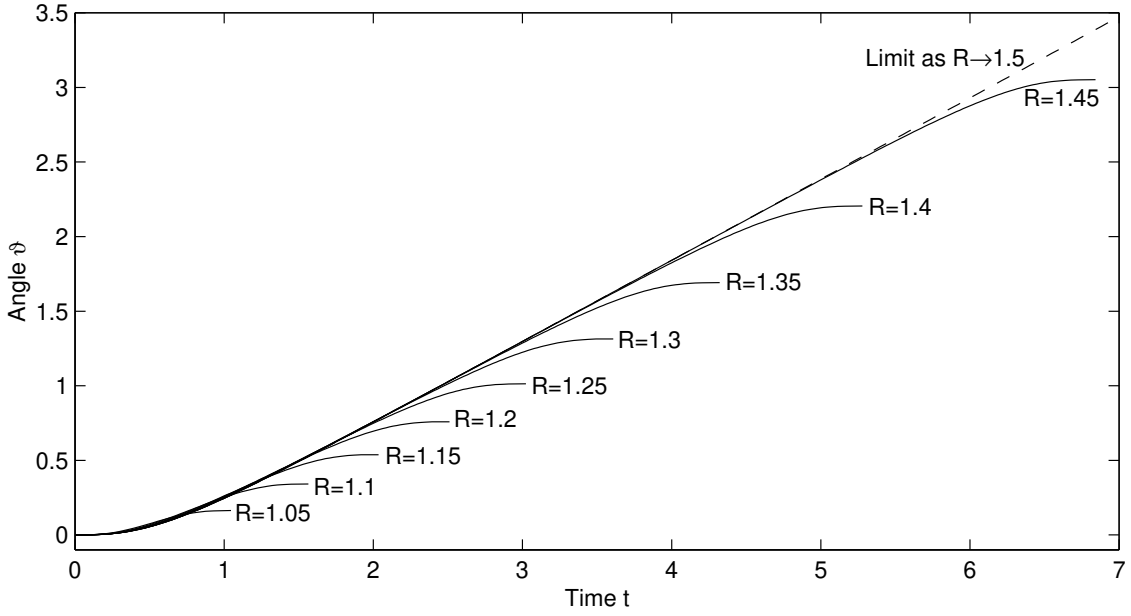

Figure 10: Arclength versus Time, for maximum radius R = 1.05 (0.05) 1.45

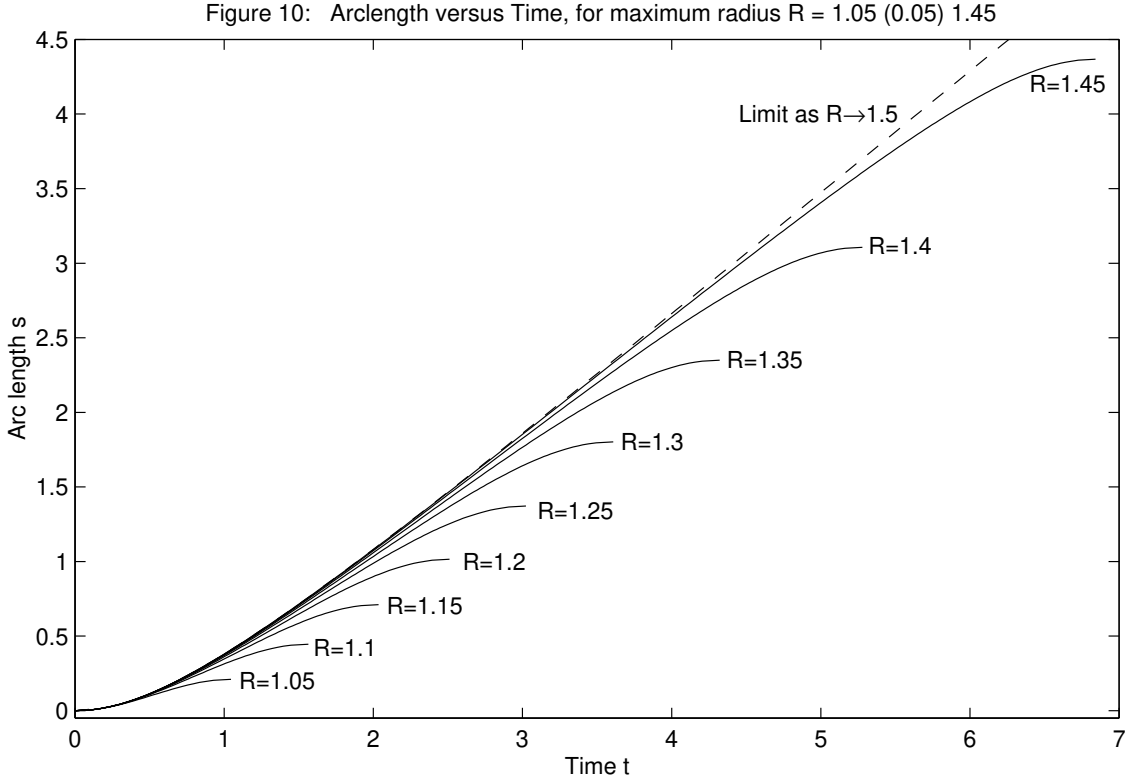

Also, in each figure there is shewn the limit of those graphs (cf. §3) as $R \nearrow \frac{3}{2}$ (and $J \searrow \frac{27}{4}$), which is the graph for the brachistochrone with $J = \frac{27}{4}$. That limit is not symmetric.

3 The Critical Brachistochrone

As $R \nearrow \frac{3}{2}$ (and $J \searrow \frac{27}{4}$), the quadratic q in (12) has its larger zero decreasing to $\frac{3}{2}$; and with $J = \frac{27}{4}$, $q\left(\frac{3}{2}\right) = 0$. Hence, with parameter $J = \frac{27}{4}$, the cubic polynomial in (2), (3) and (4) has a squared factor, as in (12); and so the elliptic integrals (2), (3) and (4) reduce to the integrals:

$$\begin{aligned} \vartheta &= \int_1^r \frac{\pm 1}{x\left(\frac{3}{2} - x\right)} \sqrt{\frac{27(x-1)}{4(x+3)}}\, \mathrm{d}x \ , \\ s &= \int_1^r \frac{\pm x}{\frac{3}{2} - x} \sqrt{\frac{x}{x+3}}\, \mathrm{d}x \ , \\ t &= \int_1^r \frac{\pm x^2}{\left(\frac{3}{2} - x\right)\sqrt{2(x-1)(x+3)}}\, \mathrm{d}x \ . \end{aligned} \tag{28}$$

Thus, this Critical Brachistochrone with $J = \frac{27}{4}$ can be expressed in terms of *elementary functions*!

When the particle starts from A at time $t = 0$, the repulsive force will make r increase with t (initially, at least); and hence the positive square root is to be used in each of the integrals (28). If $\mathrm{d}r/\mathrm{d}t$ ever became negative then it would pass through 0 at an apse at radius R, satisfying equation (6); and with $J = \frac{27}{4}$ that equation is satisfied only by $R = \frac{3}{2}$. But the factor $\left(\frac{3}{2} - x\right)$ in the denominators of the integrands in (28) makes ϑ increase unboundedly as $r \nearrow \frac{3}{2}$, (and similarly for s and t). Hence, the radius $r = \frac{3}{2}$ is never attained by the Critical Brachistochrone, and so $\mathrm{d}r/\mathrm{d}t$ never changes sign from + to -. Therefore, in the integrals (28) the positive square roots are always to be used. Unlike those bounded total brachistochrones with total angle $\geq 2\pi$, the Critical Brachistochrone does not intersect itself.

Thus, the Critical Brachistochrone spirals endlessly out from $r = 1$, winding infinitely often around the centre and approaching asymptotically the critical radius $r = \frac{3}{2}$, but never reaching it.

Taking the positive sign in the integrals (28), we get the Critical Brachistochrone expressed in terms of elementary functions:

$$\begin{aligned} \vartheta &= -2\ \arccos\left(\frac{1}{2}\sqrt{1 + \frac{3}{r}}\right) + \frac{1}{\sqrt{3}} \log\left(\frac{5r - 3 + 3\sqrt{(r-1)(r+3)}}{4}\right) \\ &\qquad - \frac{1}{\sqrt{3}} \log\left(\tfrac{3}{2} - r\right), \end{aligned} \tag{29}$$

$$\begin{aligned} s &= 2 - \sqrt{r(r+3)} + \frac{\sqrt{3}}{2}\ \log\left(\frac{2r + \frac{3}{2} + \sqrt{3r(r+3)}}{7 + 4\sqrt{3}}\right) \\ &\qquad - \frac{\sqrt{3}}{2} \log\left(\tfrac{3}{2} - r\right), \end{aligned} \tag{30}$$

$$\begin{aligned} t &= -\frac{1}{\sqrt{8}} \log\left(\frac{1 + r + \sqrt{(r-1)(r+3)}}{2}\right) - \sqrt{\frac{(r-1)(r+3)}{2}} \\ &\quad + \frac{3}{\sqrt{8}} \log\left(\frac{5r - 3 + 3\sqrt{(r-1)(r+3)}}{4}\right) - \frac{3}{\sqrt{8}} \log\left(\tfrac{3}{2} - r\right). \end{aligned} \tag{31}$$

In these expressions each term is a bounded function of r; except for the terms in $\log(\frac{3}{2}-r)$, which diverge as $r \nearrow \frac{3}{2}$. Thus the Critical Brachistochrone is bounded in radius, but it is unbounded in angle, in arclength and in time.

3.1 Picture of the Critical Brachistochrone

The Critical Brachistochrone is constructed in Figure 11, from the explicit equation (29). Note that, for $\vartheta \geq \pi$, the Critical Brachistochrone is very close to the critical radius $r = \frac{3}{2}$. Indeed, solving equation (29) for r with $\vartheta = \pi$, by using the Newton–Raphson method, we get that $r = \tilde{r} = 1{\cdot}498409827743414$ at $\vartheta = \pi$.

Figure 11. Critical Brachistochrone

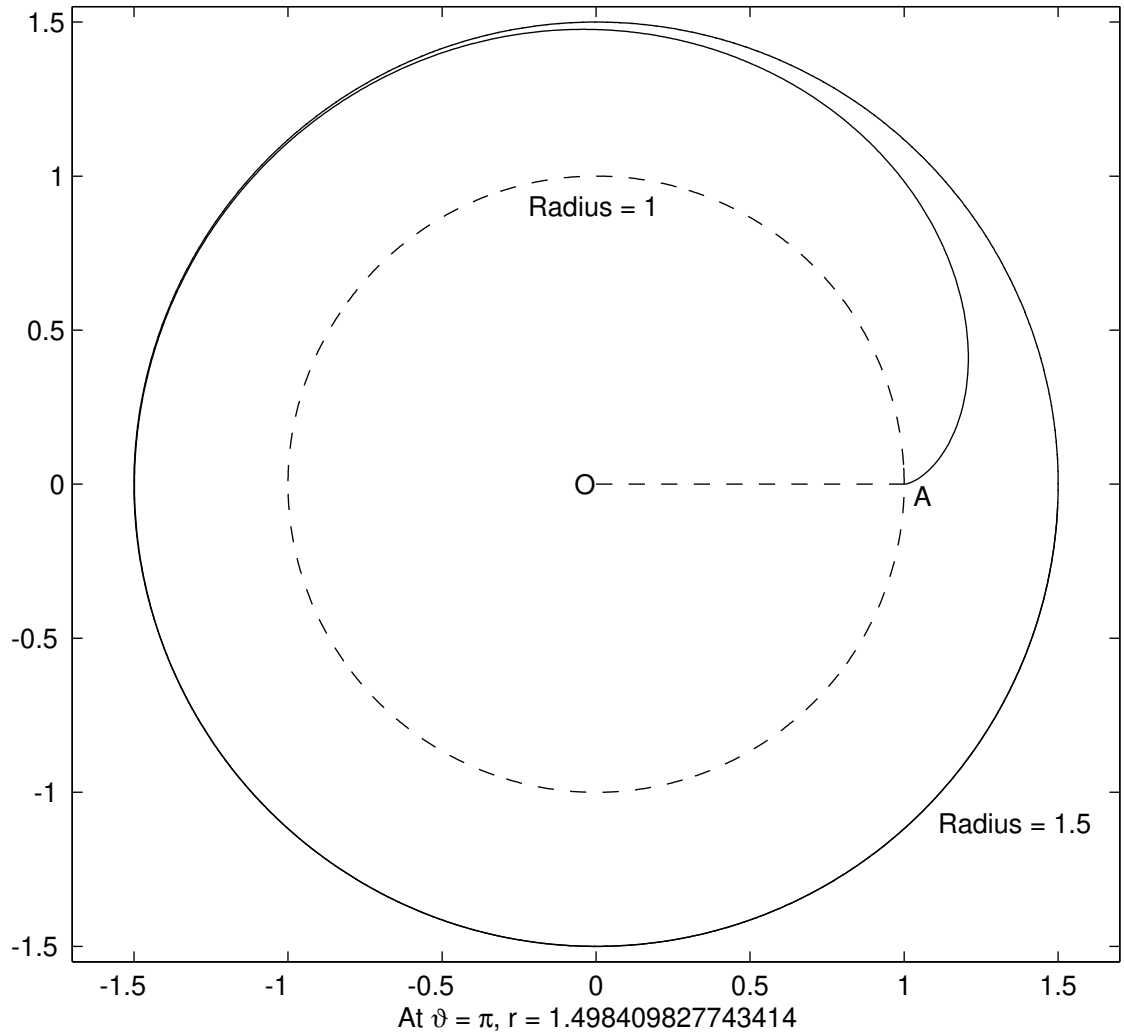

In each of Figures 1, 2 and 6 to 10 with graphs of bounded brachistochrones for $J > \frac{27}{4}$, the Critical Brachistochrone is included as the graph with $J = \frac{27}{4}$, which is the limit of those graphs as $R \nearrow \frac{3}{2}$ and $J \searrow \frac{27}{4}$. Likewise, in Figure 12 and in each of Figures 18 to 23, with graphs of unbounded brachistochrones for $J < \frac{27}{4}$, the Critical Brachistochrone is represented by the graph with $J = \frac{27}{4}$, which is the limit of those graphs as $J \nearrow \frac{27}{4}$. But the Critical Brachistochrone is not shewn in Figures 3, 4 or 5, since each of the first half–arches of the bounded brachistochrones, for R close to $\frac{3}{2}$, would be barely distinguishable from the Critical Brachistochrone.

4 Unbounded Brachistochrones

With $0 < J < \frac{27}{4} = 6{\cdot}75$ there is no apse at which $\mathrm{d}r/\mathrm{d}s = 0$, and hence ϑ, s and t each increase monotonically with r; and conversely r increases monotonically with ϑ, with s and with t. Hence, no unbounded brachistochrone intersects itself. In the elliptic integrals (2), (3) and (4), the positive sign is to be taken everywhere.

For $r > 1$, the minimum value of the cubic polynomial $c(r) = r^3 - Jr + J$ is attained at $x = \sqrt{J/3}$, so that $x < \frac{3}{2}$ for $J < \frac{27}{4}$. That minimum value is

$$c\left(\sqrt{\frac{J}{3}}\right) \;=\; \left(\frac{J}{3}\right)^{3/2} - J\left(\frac{J}{3}\right)^{1/2} + J \;=\; \frac{4J}{27\left(1+\sqrt{\frac{4J}{27}}\right)}\left(\tfrac{27}{4} - J\right) \;>\; 0, \qquad (32)$$

for all $0 < J < \frac{27}{4}$. Therefore, the cubic polyomial $c(x)$ in the denominators of (2), (3) and (4) is positive for all $x > 1$. Hence, in (2) and (3) the integrands are continuous for all $r \geq 1$; but in (4) the integrand has an integrable singularity at $r = 1$, and so it is only continuous for all $r > 1$.

4.1 Form of the Curve

As $r \nearrow \infty$ (and so $s \nearrow \infty$) then $v \nearrow \sqrt{2}$, and hence t increases unboundedly. As $x \nearrow \infty$ the integrand in (2) is asymptotically $\sqrt{J}/x^2$, and hence the integral converges as $r \nearrow \infty$. Hence, for any fixed $J < \frac{27}{4}$, ϑ converges to a least upper bound, which we call the *asymptotic angle*. With $J = 0$ the asymptotic angle is 0; and as $J \nearrow \frac{27}{4}$, inside $r = \frac{3}{2}$ the unbounded brachistochrone converges to the Critical Brachistochrone, which winds infinitely many times around the centre O. Hence, as $J \nearrow \frac{27}{4}$, the asymptotic angle increases unboundedly, with the path for $r < \frac{3}{2}$ winding unboundedly many times around the centre O.

Also, after the particle penetrates the critical radius $\frac{3}{2}$, the path there winds unboundedly many times around the centre, as $J \nearrow \frac{27}{4}$. Indeed, the increment of angle (cf. (2)) from radius r to infinity is

$$\delta(r, J) \;\stackrel{\text{def}}{=}\; \vartheta(\infty) - \vartheta(r) \;=\; \int_r^\infty \frac{\mathrm{d}x}{x\sqrt{\frac{x^3}{J(x-1)} - 1}}\,. \qquad (33)$$

For $r > \frac{3}{2}$, as $J \nearrow \frac{27}{4}$, $\delta(r, J)$ increases monotonically towards its limit with $J = \frac{27}{4}$. Thus (cf. (28) & (29)), for each fixed $r > \frac{3}{2}$,

$$\begin{aligned}
\lim_{J\nearrow 27/4} \delta(r, J) \;&=\; \int_r^\infty \frac{\mathrm{d}x}{x\sqrt{\frac{27x^3}{4(x-1)} - 1}} \\
&=\; \sqrt{\frac{27}{4}} \int_r^\infty \frac{1}{x\left(x - \frac{3}{2}\right)} \sqrt{\frac{x-1}{x+3}}\; \mathrm{d}x = \left[2\;\arccos\left(\frac{1}{2}\sqrt{1+\frac{3}{r}}\right)\right. \\
&\qquad \left. -\frac{1}{\sqrt{3}} \log\left(\frac{5r - 3 + 3\sqrt{(r-1)(r+3)}}{4}\right) + \frac{1}{\sqrt{3}} \log\left(r - \tfrac{3}{2}\right)\right]_r^\infty \\
&=\; \left[2\arccos\left(\tfrac{1}{2}\sqrt{1+\tfrac{3}{r}}\right) - \frac{1}{\sqrt{3}} \log\left(\frac{5 - \frac{3}{r} + 3\sqrt{(1-\frac{1}{r})(1+\frac{3}{r})}}{4 - \frac{6}{r}}\right)\right]_r^\infty \qquad (34)
\end{aligned}$$

and so

$$\lim_{J\nearrow 27/4}\delta(r,J) \;=\; \frac{2\pi}{3} - 2\,\arccos\left(\frac{1}{2}\sqrt{1+\frac{3}{r}}\right) + \frac{1}{\sqrt{3}}\log\left(\frac{5r-3+3\sqrt{(r-1)(r+3)}}{8}\right) - \frac{1}{\sqrt{3}}\log\left(\tfrac{3}{2}-r\right)\,. \tag{35}$$

Therefore, as $r \searrow \frac{3}{2}$, the limit (as $J \nearrow \frac{27}{4}$) of the angle increment outside the critical radius $\frac{3}{2}$ is asymptotically $C - [\log(r-\frac{3}{2})]/\sqrt{3}$ (where $C = \pi/3 - \log(9/8)/\sqrt{3}$), and that grows unboundedly.

Thus, as $J \nearrow \frac{27}{4}$, the path close to the critical radius $\frac{3}{2}$ winds unboundedly many times around the centre, both inside and outside that critical radius.

4.1.1 Angle Between Tangent and Radius Vector

Denote by $\xi(r)$ the angle between the tangent and the radius vector, so that (cf. Tee, 1999, (18))

$$\sin\xi \;=\; \frac{r\,\mathrm{d}\vartheta}{\mathrm{d}s} \;=\; \frac{Kv}{r} \;=\; \frac{K}{r}\sqrt{\frac{2(r-1)}{r}} \;=\; \sqrt{J(r^{-2}-r^{-3})}\,. \tag{36}$$

At the startpoint with $r = 1,\ \xi(1) = 0$.

The particle never moves at a right–angle to the radius vector for an unbounded brachistochrone — but (for each $J < \frac{27}{4}$), ξ will be maximized at that radius r for which $r^{-2} - r^{-3}$ is maximized. Now,

$$\frac{\mathrm{d}}{\mathrm{d}r}(r^{-2}-r^{-3}) \;=\; -2r^{-3}+3r^{-4} \;=\; \frac{2}{r^4}\left(\tfrac{3}{2}-r\right)\,. \tag{37}$$

Therefore, as r increases from 1 to $\frac{3}{2}$, $(r^{-2}-r^{-3})$ increases from 0 to its maximum value of $\frac{4}{27}$, and as r increases from $\frac{3}{2}$ then ξ decreases.

Hence the maximum angle between the tangent and the radius vector is

$$\xi\left(\tfrac{3}{2}\right) \;=\; \arcsin\sqrt{\tfrac{4}{27}J}\,. \tag{38}$$

As $J \nearrow \frac{27}{4}$, then $\xi\left(\frac{3}{2}\right) \nearrow \frac{1}{2}\pi$.

Thus, for each unbounded brachistochrone the path spiralling outwards will be closest to being circular at the critical radius $r = \frac{3}{2}$. For J slightly less than $\frac{27}{4}$, with the path winding around O more than once, the successive turns of the spiral are there closest together, as in Figure 16 with $J = 6{\cdot}749996$.

As $r \nearrow \infty$ then $\xi \searrow 0$. Hence, as the particle moves outwards, its direction becomes ever closer to radial and the brachistochrone converges asymptotically to the radius vector at its asymptotic angle.

4.2 Inversion of Unbounded Brachistochrones

It is difficult to make effective pictures of the unbounded brachistochrones for $r \gg 1$, since they fill the entire plane outside the critical circle $r = \frac{3}{2}$. Accordingly, we shall

represent them for $r \gg 1$ by their images generated by inversion in the unit circle, with each point (r, ϑ) getting mapped onto $(1/r, \vartheta)$. Thus, the exterior of the unit circle gets mapped onto its interior.

Under inversion, each line through O gets mapped onto itself (with O and the point at infinity getting interchanged), and the transformation is continuous along all smooth curves not passing through O. Each line not passing through O gets mapped onto a circle through O, and inversely. Each circle not passing through O gets mapped onto a circle, with each circle of radius $r > 0$ centred on O getting mapped onto the circle of radius $1/r$, centred on O. Also, the transformation is conformal, so that angles of intersection of curves (not at O) are preserved under inversion.

Substitute $\lambda = 1/r$ and $z = 1/x$ in (2) (with positive sign everywhere), so that we get angle ϑ expressed as an elliptic integral of λ:

$$\vartheta \;=\; \int_{\lambda}^{1} \sqrt{\frac{J(1-z)}{Jz^3 - Jz^2 + 1}}\; \mathrm{d}z \;. \tag{39}$$

The cubic polynomial in the denominator is the inverse polynomial of $c(x) = x^3 - Jx + J$ in (5); and we have seen that for $J < \frac{27}{4}$, $c(x) > 0$ for all $x \geq 1$. Therefore the integrand in (39) is continuous for all $z \in [0, 1]$, and hence that integral can be evaluated numerically.

As $r \nearrow \infty$ the brachistochrone converges asymptotically to the radius vector at its asymptotic angle. Hence, that radius vector is the tangent to the inverse image at the centre.

4.3 Angle as a Function of Radius for Unbounded Brachistochrones

For unbounded brachistochrones, positive signs are to be taken in the elliptic integrals (2), (3) and (4).

The elliptic integral (2) has a singularity in the derivative of the integrand at $x = 1$. That near–singularity may be eliminated by an appropriate change of variable, to produce a smooth integrand which is suitable for numerical quadrature by Romberg integration for all $r \geq 1$.

4.3.1 Elimination of Near–singularities

Substitute

$$x \;=\; x(y) \;=\; 1 + y^2, \tag{40}$$

so that $y = \sqrt{x-1}$ and $\mathrm{d}x = 2y\;\mathrm{d}y$. Hence, the elliptic integral (2) becomes

$$\vartheta \;=\; \int_{0}^{\sqrt{r-1}} \frac{2\sqrt{J}\; y^2}{(1+y^2)\sqrt{(1+y^2)^3 - Jy^2}}\; \mathrm{d}y \;. \tag{41}$$

And this transformed integral is suitable for Romberg integration with respect to y.

In (39) for the inverse image, the factor $\sqrt{1-z}$ in the integrand results in the integrand having unbounded derivative as $z \nearrow 1$. In order to remove that near–singularity substitute $z = 1 - u^2$, so that $u = \sqrt{1-z}$ and (39) becomes

$$\vartheta(r) \;=\; \int_{0}^{\sqrt{1-1/r}} 2u^2 \sqrt{\frac{J}{1 - Ju^2(1-u^2)^2}}\; \mathrm{d}u \;. \tag{42}$$

In particular, the asymptotic angle (at $r = \infty$ and $\lambda = 0$) is

$$\vartheta(\infty) \;=\; \int_0^1 2u^2 \sqrt{\frac{J}{1 - Ju^2(1-u^2)^2}}\; \mathrm{d}u \;. \tag{43}$$

And these transformed integrals are suitable for Romberg integration with respect to u.

4.3.2 Pictures of Unbounded Brachistochrones

Figure 12 shews the unbounded brachistochrones for $J = 0\ (0{\cdot}5)\ 6{\cdot}5$. The unbounded brachistochrone with $J = 0$ is the radius vector $\vartheta = 0$ with $r \geq 1$, as in (Tee, 1999, (49)).

Figure 12. Unbounded Brachistochrones, for J = 0 (0.5) 6.5 and 6.75

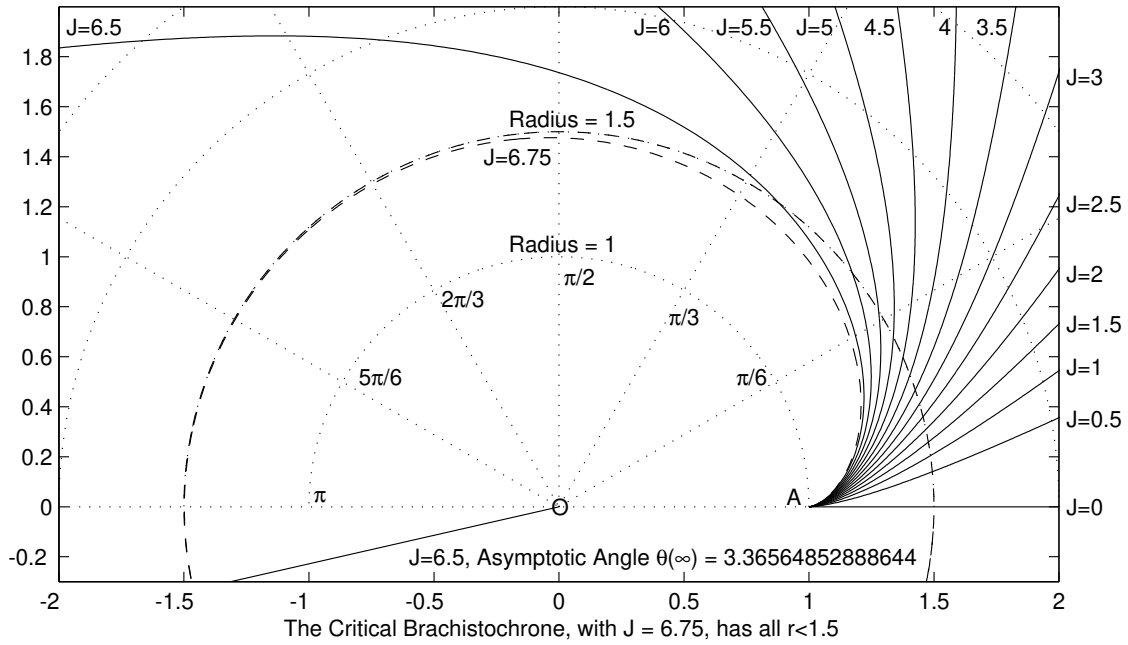

If brachistochrones were plotted for equidistant values of K, then they would asymptotically become equally spaced as $r \searrow 1$. But these brachistochrones are plotted for $J = 0,\ 0{\cdot}5, 1,\ 1{\cdot}5$ *et cetera*, where $J = 2K^2$. Accordingly, in Figure 12 the spacings between successive brachistochrones (e.g. on the circle $r = 1{\cdot}5$) are approximately in the ratio of $1 : (\sqrt{2}-1) : (\sqrt{3}-\sqrt{2}) : (2-\sqrt{3}) : \ \ldots$. Also, there is shewn the limit of those unbounded brachistochrones for $r < \frac{3}{2}$ as $J \nearrow 6{\cdot}75$, which is the (bounded) Critical Brachistochrone with $J = 6{\cdot}75$. Figure 13 shews the inverses of those unbounded brachistochrones. For $J = 6{\cdot}5$ the tangent at the centre to the inverse curve is drawn, at the asymptotic angle for that brachistochrone of $\vartheta(\infty) = 3{\cdot}36564852888644$.

Figure 14 shews the unbounded brachistochrones for $J = 6{\cdot}5\ (0{\cdot}0125)\ 6{\cdot}7375$, and Figure 15 shews the inverses of those unbounded brachistochrones. For $J = 6{\cdot}7375$ the tangent at the centre to the inverse curve is drawn, at the asymptotic angle for that brachistochrone of $\vartheta(\infty) = 5{\cdot}13242329246298$.

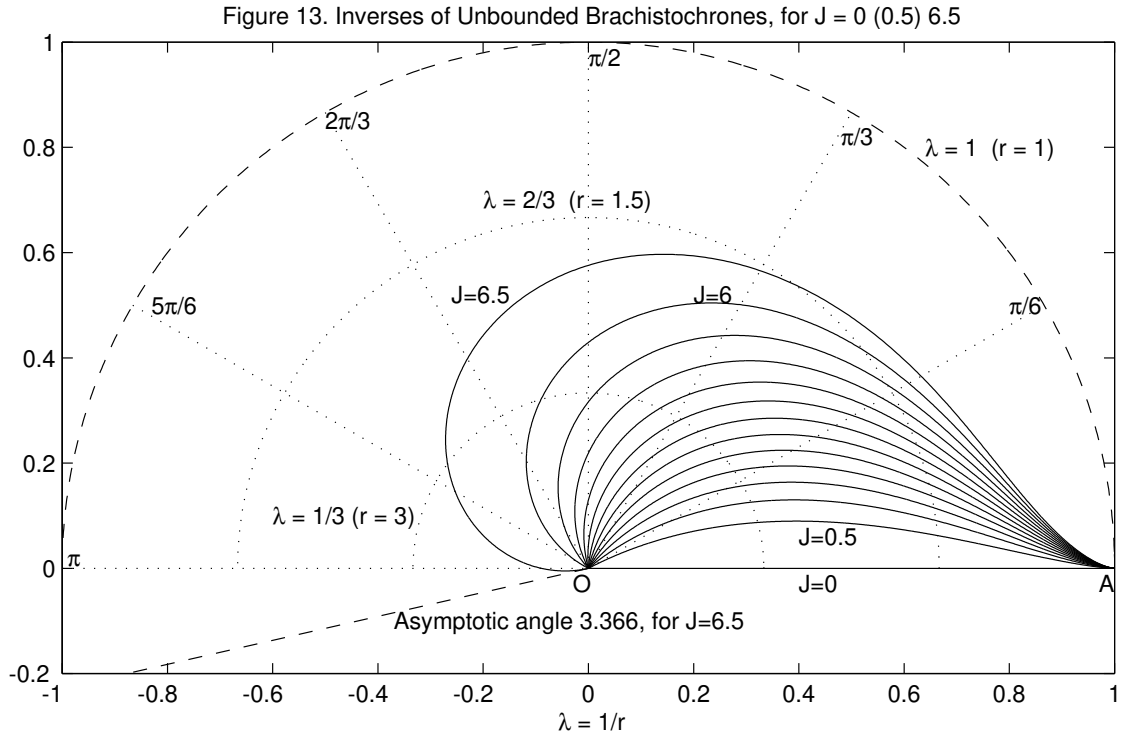

Figure 16 shews the unbounded brachistochrone for $J = 6{\cdot}7499996$, and Figure 17 shews the inverse of that unbounded brachistochrone. The tangent at the centre to the inverse curve is drawn, at the asymptotic angle for that brachistochrone of $\vartheta(\infty) = 9{\cdot}78114831817315$.

All graphs in this paper were drawn by the MATLAB 5 procedure "plot", which connects each point to its successor by a straight segment. When the interval $1 \leq r \leq 3$ was divided into 8000 equal sub-intervals of $\frac{1}{4000}$, near $r = 1{\cdot}5$ the increment in ϑ between successive values of r was large enough for the graph in Figure 16 to appear visibly polygonal. Accordingly, Figure 16 was drawn with the interval $1 \leq r \leq 3$ divided into 16000 equal sub-intervals of $\frac{1}{8000}$, and Figure 17 was drawn with the interval $0 \leq \lambda \leq 1$ divided into 16000 equal sub-intervals of $\frac{1}{16000}$, which did produce smooth curves.

4.4 Arclength as a Function of Radius for Unbounded Brachistochrones

The integrand in (3) is smooth, and hence $s(r)$ can readily be numerically evaluated for $r \geq 1$, by Romberg integration with respect to x.

Figure 14. Unbounded Brachistochrones, for J = 6.5 (0.0125) 6.7375

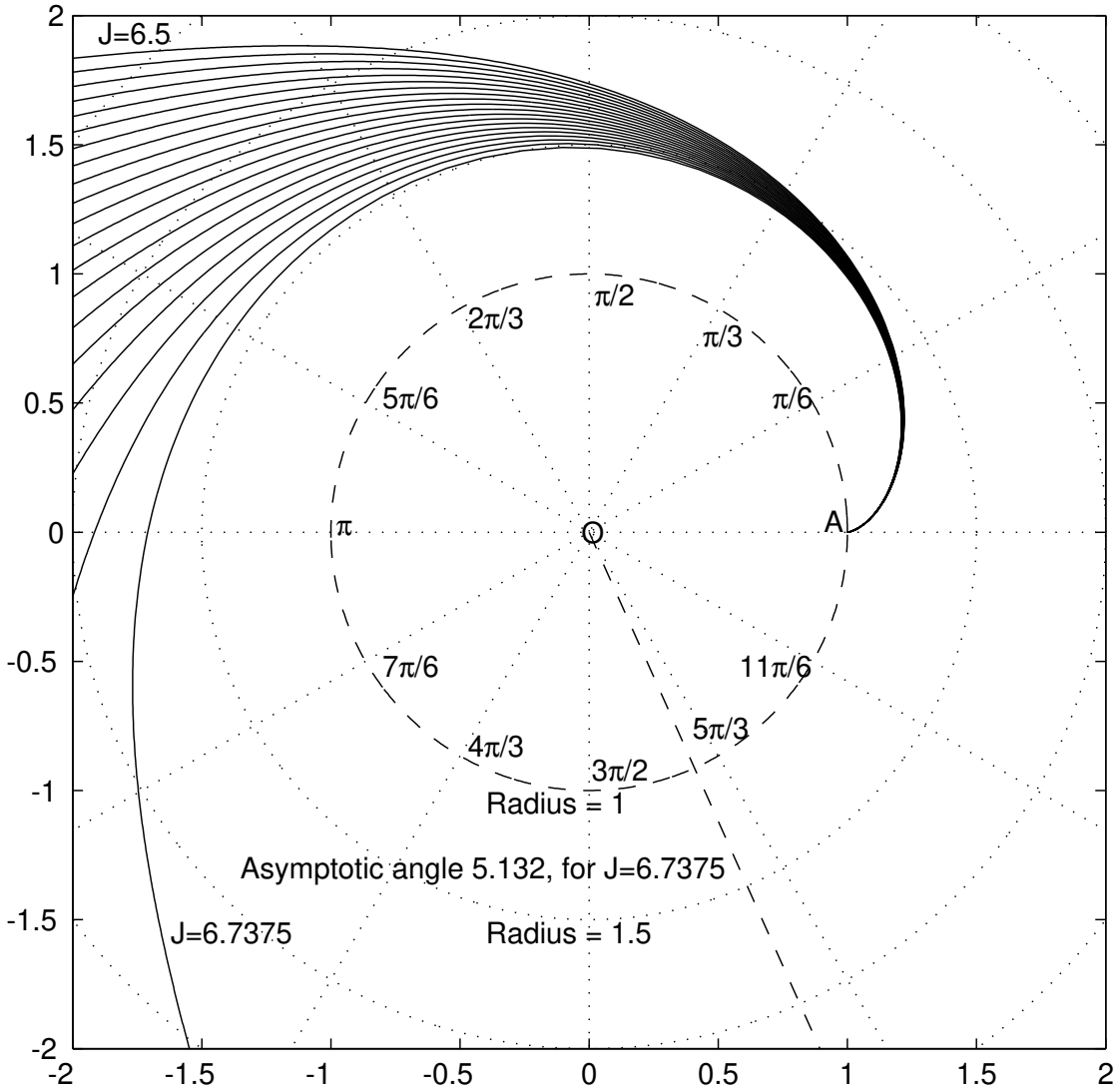

4.4.1 Graphs of Radius versus Arclength

For each unbounded brachistochrone, the angle ξ between the tangent and the radius vector attains its maximum at $r = \frac{3}{2}$. Since $\mathrm{d}r/\mathrm{d}s = \cos\xi$, it follows that $\mathrm{d}r/\mathrm{d}s$ attains its minimum value at the critical radius $r = \frac{3}{2}$; and hence each graph of r versus s has exactly one point of inflexion, at $r = \frac{3}{2}$.

Figure 15. Inverses of Unbounded Brachistochrones, for J = 6.5 (0.0125) 6.7375

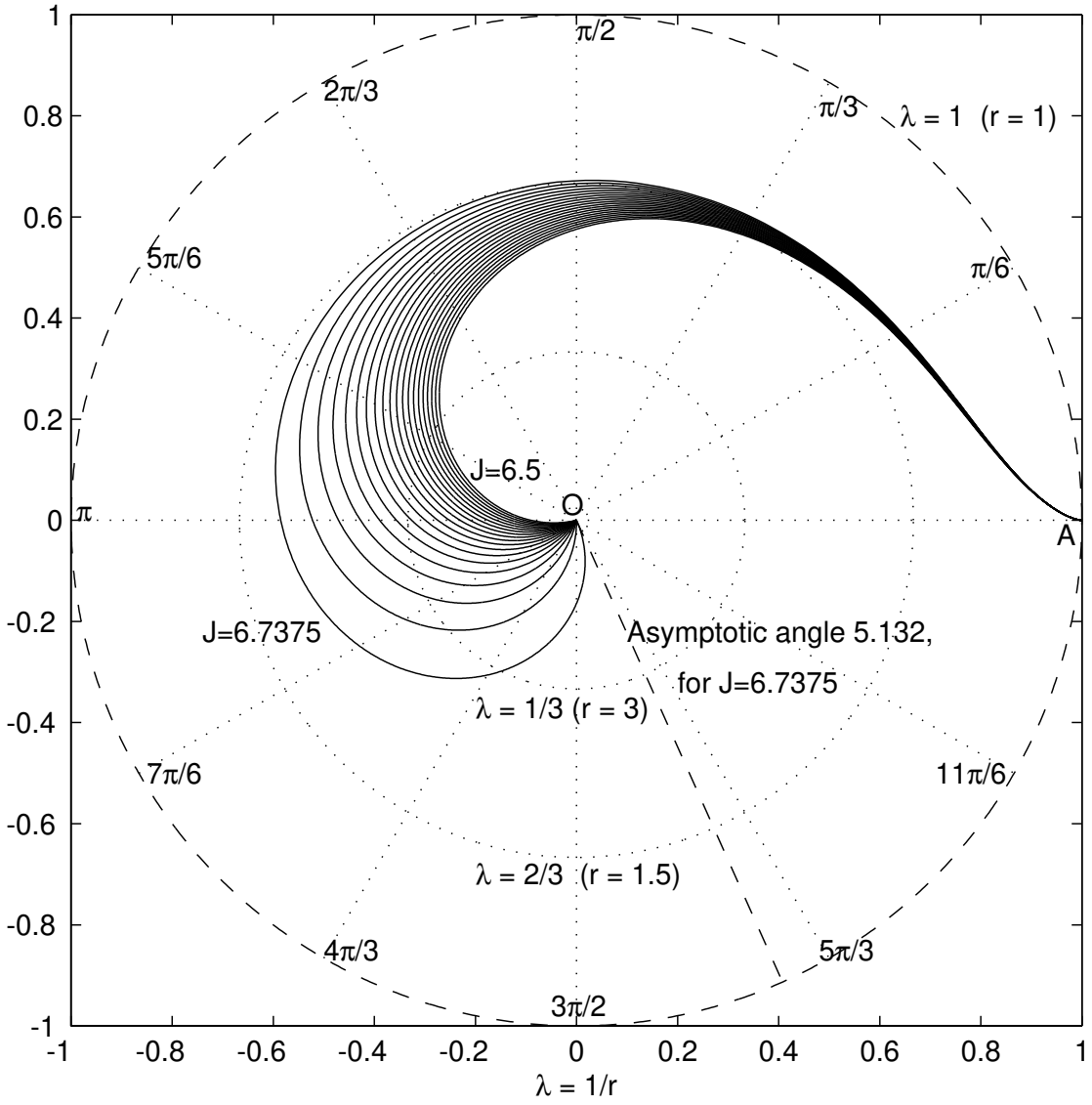

Figure 18 shews graphs of r versus s, for the unbounded brachistochrones with $J = 0\ (0{\cdot}5)\ 6{\cdot}5$. In Figure 18 (and also in Figure 6) the limiting graph for the Critical Brachistochrone, with $J = 6{\cdot}75$, is given explicitly by (30).

The graph for $J = 0$, representing radial motion, has the equation $r = s - 1$. The line $r = 1{\cdot}5$ is the asymptote for the Critical Brachistochrone graph; and also it is the locus of the points of inflexion on the graphs. The inflexion is seen clearly on the graph for $J = 6{\cdot}5$.

As $r \nearrow \infty$ each unbounded brachistochrone with $J < 6{\cdot}75$ converges asymptotically to the radius vector at the asymptotic angle for J. Hence, each graph has slope increasing with s (and r) and converging to 1.

Figure 16. Unbounded Brachistochrone, for J = 6.749996

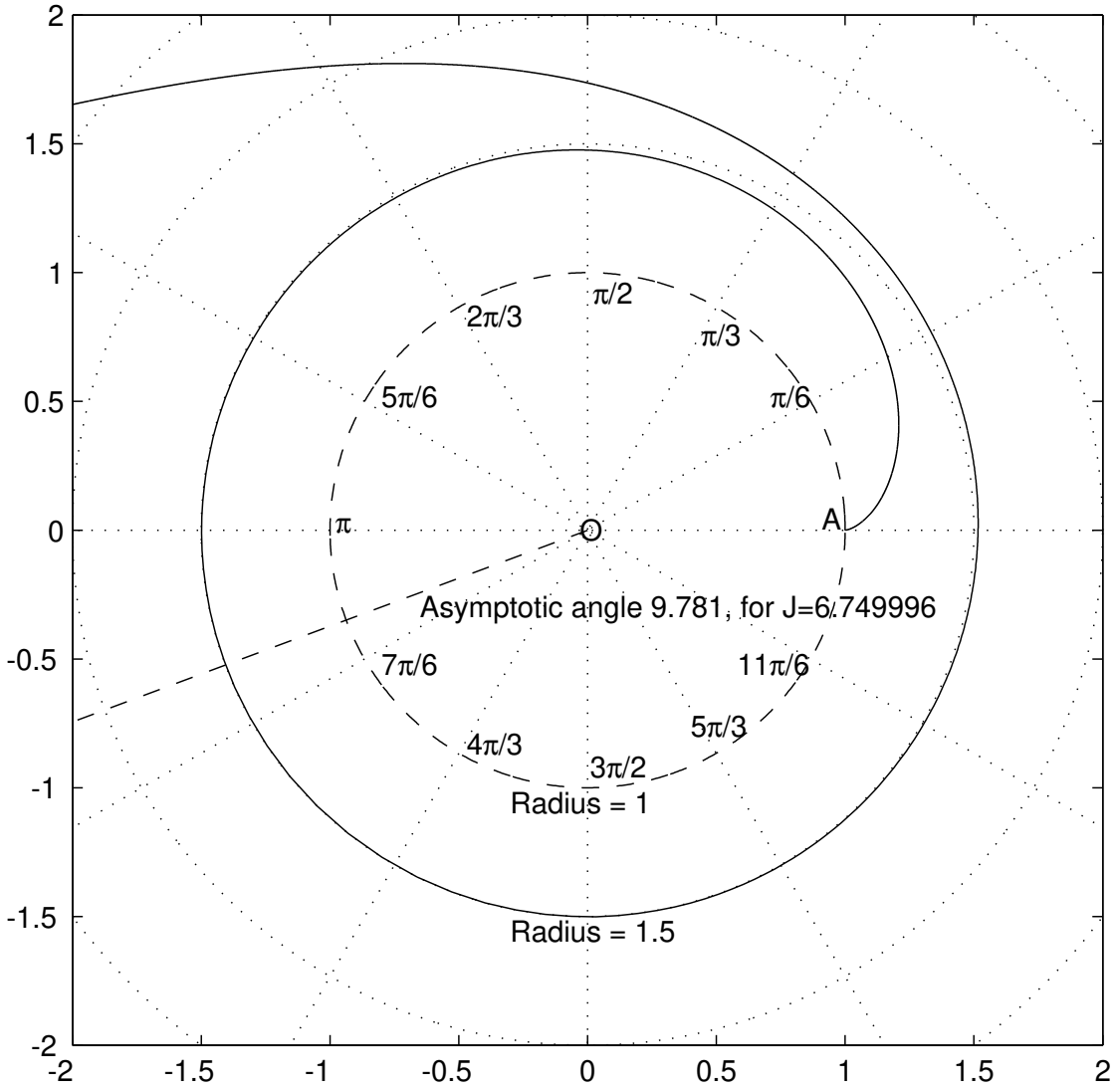

4.5 Time as a Function of Radius for Unbounded Brachistochrones

The elliptic integral (4) has an integrable singularity at $x = 1$. That singularity may be eliminated by an appropriate change of variable, to produce a smooth integrand which is suitable for numerical quadrature by Romberg integration for all $r \geq 1$.

4.5.1 Elimination of Singularity

With the substitution (40), the elliptic integral (4) becomes

$$t \;=\; \int_0^{\sqrt{r-1}} \frac{\sqrt{2}(1+y^2)^2}{\sqrt{(1+y^2)^3 - Jy^2}}\,\mathrm{d}y \;. \tag{44}$$

And this transformed integral is suitable for Romberg integration with respect to y.

Figure 17. Inverse of Unbounded Brachistochrone, for J = 6.749996

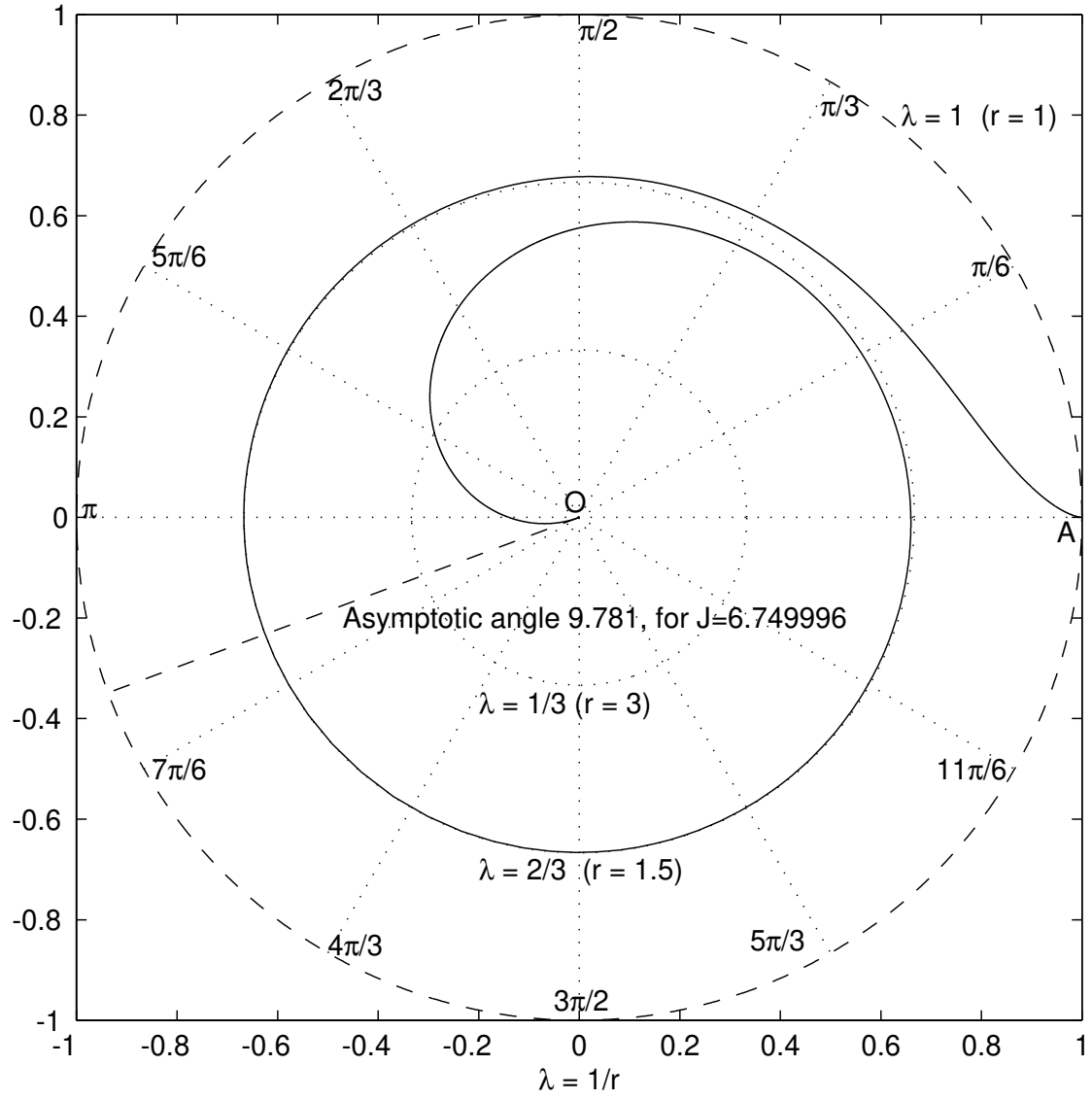

Figure 18: Radius versus Arclength, for J=0 (0.5) 6.5 and 6.75

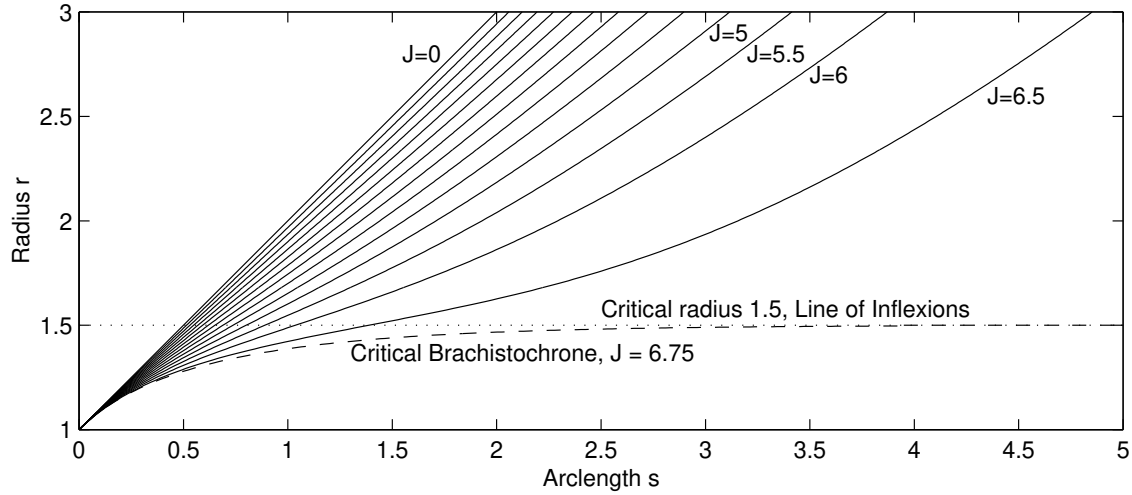

4.5.2 Graphs of Radius versus Time

Figure 19 shews graphs of r versus t, for the unbounded brachistochrones with $J = 0$ (0·5) 6·5 . In Figure 19 (and also in Figure 7), the limiting graph for the Critical Brachistochrone with $J = 6{\cdot}75$ is given explicitly by (31).

The graph for $J = 0$, representing radial motion (cf. Tee, 1999, (49)), has the equation $t = [\sqrt{r(r-1)} + \log(\sqrt{r} + \sqrt{r-1})]/\sqrt{2}$. The line $r = 1{\cdot}5$ is the asymptote for the Critical Brachistochrone.

As $r \nearrow \infty$ each unbounded brachistochrone with $J < 6{\cdot}75$ converges asymptotically to the radius vector at the asymptotic angle for J, and the speed of the particle increases asymptotically (1) towards $\sqrt{2}$. Hence, each graph has slope asymptotically increasing towards $\sqrt{2}$.

Figure 19: Radius versus Time, for J=0 (0.5) 6.5 and 6.75

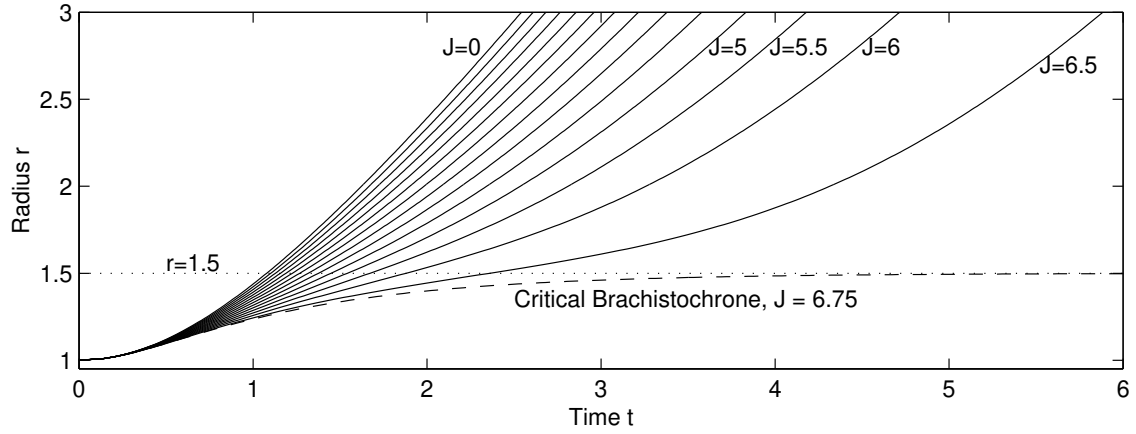

4.6 Angle, Arclength and Time for Unbounded Brachistochrones

Each of ϑ, s and t is a computable function of r. Accordingly, for various values of J, each of the three relations between pairs of these variables can be represented by a graph, with r as the parameter for computing values of the chosen pair of variables.

4.6.1 Relation between Arclength and Angle

Figure 20 shews graphs of ϑ versus s, for the unbounded brachistochrones with $J = 0$ (0·5) 6·5 . For $J < 6{\cdot}75$, as $s \nearrow \infty$ each graph converges towards its horizontal asymptote, with $\vartheta(r) \nearrow \vartheta(\infty)$ for that J.

In Figure 20 (and also in Figure 8) the graph for the Critical Brachistochrone with $J = 6{\cdot}75$ is given by (29) and (30), with r as parameter. As $s \nearrow \infty$, the particle spirals asymptotically towards motion on the circle $r = \frac{3}{2}$. Therefore, on the Critical Brachistochrone,

$$\lim_{s\to\infty} \frac{\mathrm{d}\vartheta}{\mathrm{d}s} \;=\; \frac{2}{3}\,. \tag{45}$$

Figure 20: Angle versus Arclength, for J = 0 (0.5) 6.5 and 6.75

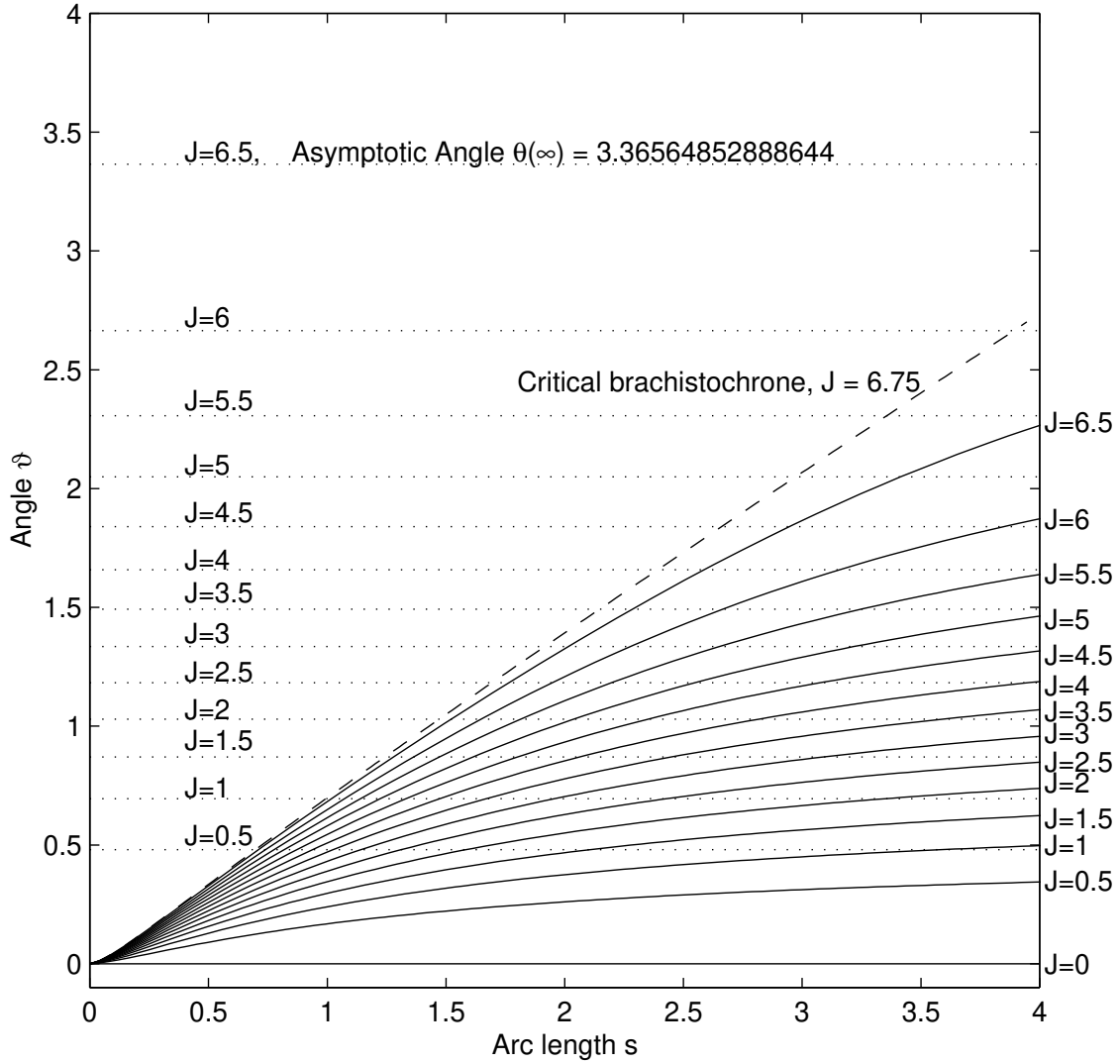

4.6.2 Relation between Time and Angle

Figure 21 shews graphs of ϑ versus t, for the unbounded brachistochrones with $J = 0\ (0{\cdot}5)\ 6{\cdot}5$. For $J < 6{\cdot}75$, as $t \nearrow \infty$ each graph converges towards its horizontal asymptote, with $\vartheta(t) \nearrow \vartheta(\infty)$ for that J.

In Figure 21 (and also in Figure 9) the graph for the Critical Brachistochrone with $J = 6{\cdot}75$ is given by (29) and (31), with r as parameter. As $t \nearrow \infty$, the particle spirals asymptotically towards uniform motion on the circle $r = \frac{3}{2}$ with speed $v\left(\frac{3}{2}\right) = \sqrt{\frac{2}{3}}$. Therefore, on the Critical Brachistochrone,

$$\lim_{t\to\infty} \frac{\mathrm{d}\vartheta}{\mathrm{d}t} \;=\; \frac{\sqrt{2/3}}{(3/2)} \;=\; \sqrt{\frac{8}{27}} \;=\; 0{\cdot}54433105395181736\ . \tag{46}$$

Figure 21: Angle versus Time, for J = 0 (0.5) 6.5 and 6.75

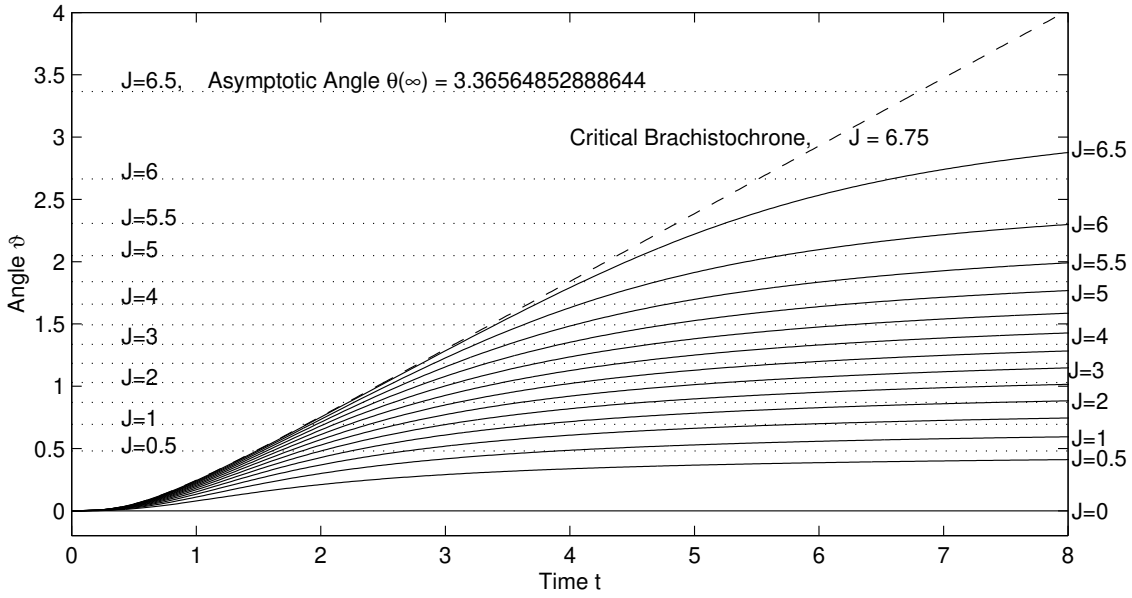

Figure 22: Arclength versus Time, for J = 0 (0.5) 6.5 and 6.75

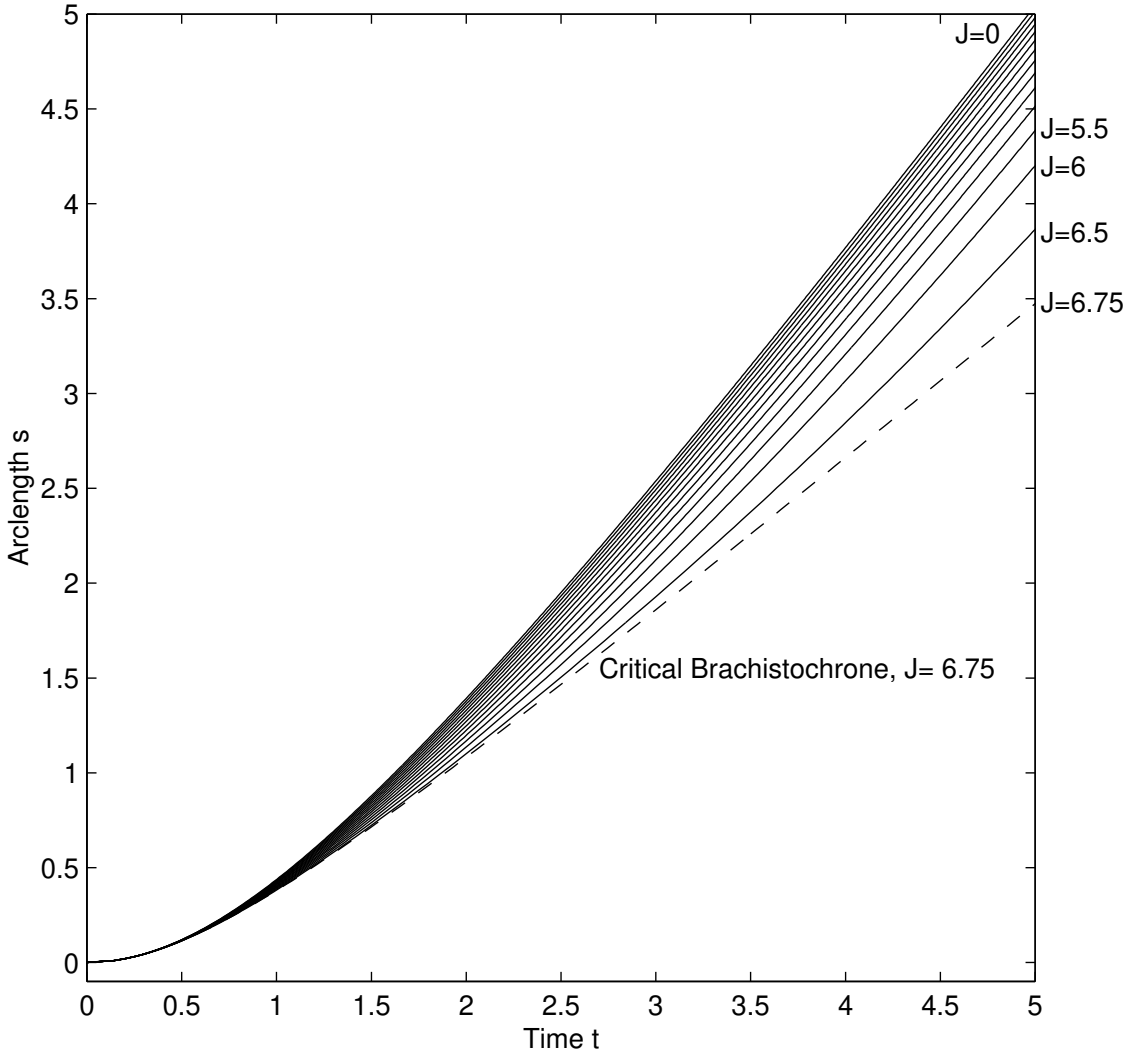

4.6.3 Relation between Arclength and Time

Figure 22 shews graphs of s versus t, for the unbounded brachistochrones with $J = 0$ (0·5) 6·5 . For $J = 0$ with radial motion, $s = r - 1$; and hence the graph is that for $J = 0$ in Figure 19, shifted down by 1. For $J < 6{\cdot}75$, as $t \nearrow \infty$ the particle's speed $v \nearrow \sqrt{2}$, and hence on each graph the slope increases asymptotically towards $\sqrt{2}$.

In Figure 22 (and also in Figure 10) the graph for the Critical Brachistochrone with $J = 6{\cdot}75$ is given by (30) and (31), with r as parameter. As $t \nearrow \infty$, the particle spirals asymptotically towards uniform motion on the circle $r = \frac{3}{2}$ with speed $v\left(\frac{3}{2}\right) = \sqrt{\frac{2}{3}}$. Therefore, on the Critical Brachistochrone,

$$\lim_{t\to\infty} \frac{\mathrm{d}s}{\mathrm{d}t} \;=\; \sqrt{\frac{2}{3}} \;=\; 0{\cdot}81649658092272603\ . \tag{47}$$

5 Critical Brachistochrone as Separatrix of Bounded and Unbounded Brachistochrones

Figure 23, with rectangular Cartesian axes for ϑ and r, shews graphs for the unbounded brachistochrones with $J = 0$ (0·5) 6·5, the Critical Brachistochrone with $J = 6{\cdot}75$, the bounded brachistochrones with $J = 7$ (1) 13, and the apsidal locus. For each $\vartheta > 0$, the first half–arches of (open) bounded brachistochrones are confined to the range of r between the Apsidal Locus and the Critical Brachistochrone,

Figure 23: Brachistochrones for J = 0 to 13, with Apsidal Locus

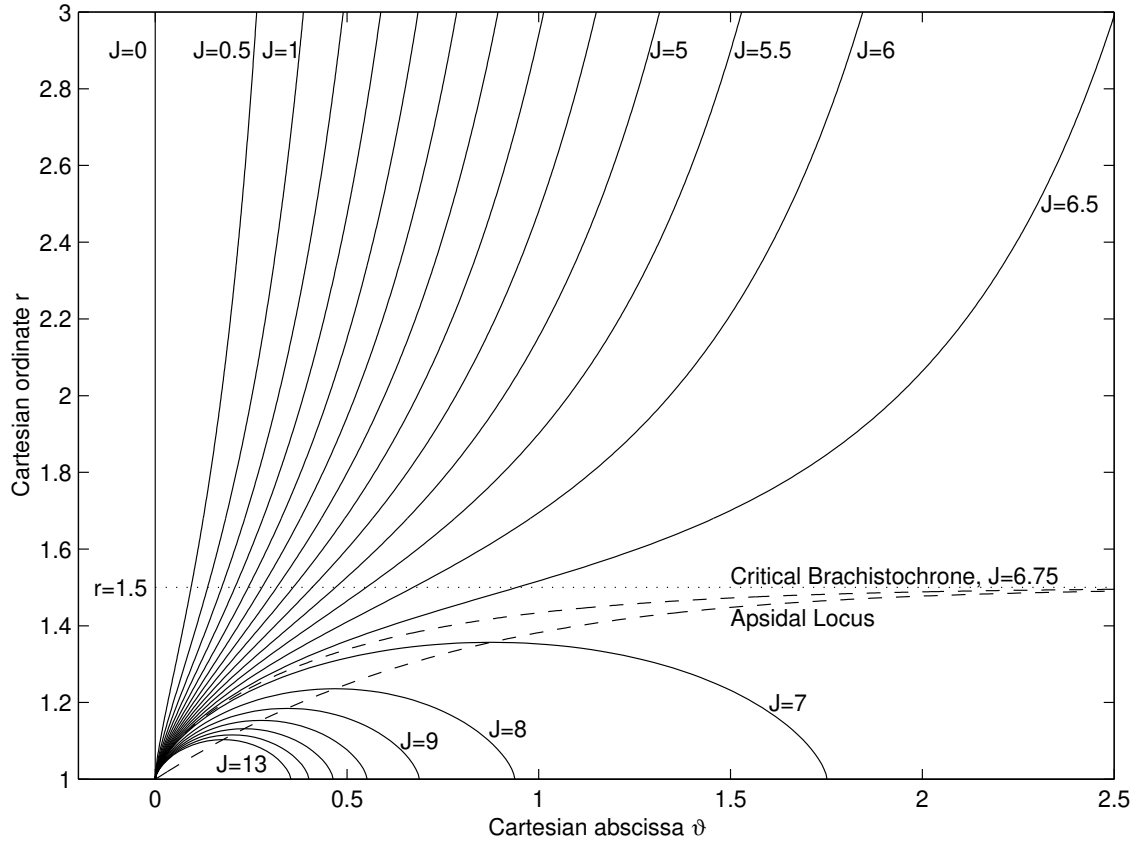

and the second half–arches are confined between $r = 1$ and the Apsidal Locus. For $J > 6{\cdot}75$, Vieta's method (11) is used to compute R, then for the first half–arch ϑ is computed by (21), and then for the second half–arch ϑ is computed by (16). The graph for each bounded brachistochrone is symmetric about the line $\vartheta = \Theta(R, R)$, the apsidal angle. For each unbounded brachistochrone, as $r \nearrow \infty$, ϑ converges to $\vartheta(\infty)$ for that J.

For brachistochrones at fixed $r \geq 1$, equations (2), (3) and (4) (each taking the positive square root) shew that each of ϑ, s and t is a continuous and strictly increasing function of J. That result holds for all $r \geq 1$ on unbounded brachistochrones with $0 \leq J < \frac{27}{4}$; and for $1 \leq r < \frac{3}{2}$ it holds also at $J = \frac{27}{4}$ (on the Critical Brachistochrone), and also on the first half–arches of bounded brachistochrones with $J \geq \frac{r^3}{r-1} > \frac{27}{4}$. These results are illustrated in Figures 1, 3, 4, 5, 11, 12, 14 and 16 for ϑ, in Figures 6 and 18 for s, and in Figures 7 and 19 for t.

However, reasoning similar to that in (Tee, 1999, (83)) shews that, for $J \geq \frac{r^3}{r-1} > \frac{27}{4}$, each of ϑ, s and t is a continuous decreasing function of J on the second half–arches of bounded brachistochrones, where the negative square roots are taken in (2), (3) and (4). Also, the apsidal angle $\Theta(R, R)$ is a decreasing function of J.

For total angle $\vartheta > 0$, r is a decreasing function of J, and J is a decreasing function of r.

Therefore, in the planes with Cartesian coordinates (ϑ, r), (s, r) and (t, r), graphs for distinct brachistochrones never intersect at any point (other than the startpoint), and no graph for any brachistochrone intersects itself. (Note, however, that Figure 8 shews the graphs with $R = 1{\cdot}15$ and $R = 1{\cdot}2$ intersecting in the (s, ϑ) plane.) Hence, in each of those 3 Cartesian planes (without the startpoint), the Critical Brachistochrone ($J = \frac{27}{4}$) separates the unbounded brachistochrones ($0 \leq J < \frac{27}{4}$) from the bounded brachistochrones ($J > \frac{27}{4}$). This separation is illustrated in Figure 6 and Figure 18 for (r, s), in Figure 7 and Figure 19 for (r, t), and in Figure 23 for (r, ϑ).

6 Infinite Family of Brachistochrones Through Two Points

Thus, for any point B at (ρ, ψ), with $\rho \geq 1$, in the plane OAB there is exactly one brachistochrone ending at B with total angle ψ. However, if ψ is any nonzero multiple of π, the plane curve can be rotated through any angle about OA, giving an uncountable infinity of brachistochrones with the same passage time.

But, in physical space with polar coordinates (r, ϑ), each physical point (r, ϑ) coincides with the physical points $(r, \vartheta + 2k\pi)$, for all integers k. Hence, each complete bounded brachistochrone with total angle $\geq 2\pi$ intersects itself, as in Figure 3, Figure 4 and Figure 5. For all $r \geq 1$, any point on a brachistochrone with total angle there of ϑ is also on brachistochrones with total angle there of $\vartheta + 2k\pi$, for every integer k.

If $r \geq \frac{3}{2}$ then each brachistochrone through C at (r, ϑ) must be unbounded, with $J < \frac{27}{4}$. For each integer k there will be an unbounded brachistochrone through C with total angle $\vartheta + 2k\pi$, which winds positively k times around O from the total angle ϑ, while staying close to $r = \frac{3}{2}$ (as in Figure 5 and Figure 16).

For $1 \leq r < \frac{3}{2}$, if the Critical Brachistochrone has total angle $> \vartheta$ at radius r, then in Figure 23 C is to the left of the graph for the Critical Brachistochrone; and hence the brachistochrone with total angle ϑ at radius r must be unbounded,

with $J < \frac{27}{4}$. If the Critical Brachistochrone has total angle $< \vartheta$ at radius r, then in Figure 23 C is to the right of the graph for the Critical Brachistochrone; and hence the brachistochrone with total angle ϑ at radius r must be bounded, with $J > \frac{27}{4}$. If C is on the Critical Brachistochrone then $J = \frac{27}{4}$ for that total angle ϑ. But, for each integer k the point C in physical space is traversed also by brachistochrones with total angle $\vartheta + 2k\pi$, each of which could be unbounded, critical or bounded.

In each case, as $k \nearrow \infty$ or $k \searrow -\infty$, then $J \to \frac{27}{4}$.

6.1 Global Minimum Passage Time

With fixed $r \geq 1$, t is an increasing function of ϑ. For, consider separately the region above (or on) the apsidal locus in Figure 23, and the region below it. Above (or on) the apsidal locus in Figure 23, each brachistochrone is either unbounded or critical, or else it ends on a (closed) first half–arch of a bounded brachistochrone. In each case, J is an increasing function of ϑ; and with fixed r and the positive square root taken in (4), t is an increasing function of J, and hence an increasing function of ϑ. Below the apsidal locus in Figure 23, on second–halfarches of bounded brachistochrones, $\mathrm{d}t/\mathrm{d}J < 0$ and $\mathrm{d}\vartheta/\mathrm{d}J < 0$ (cf. §5); and hence $\mathrm{d}t/\mathrm{d}\vartheta > 0$. Thus, for fixed r, t is an increasing function of ϑ.

With OA as the axis $\vartheta = 0$, for any spatial point B (not at O), the direction of increasing ϑ can be chosen so that the polar coordinates of B are (ρ, ψ), where $\rho \geq 0$ and $0 \leq \vartheta \leq \pi$. If $\rho \geq 1$ then there is a unique brachistochrone with endpoint B and total angle ψ — unless $\psi = \pi$, in which case the brachistochrone AB can be rotated through any angle around OA.

With $\psi < \pi$, the brachistochrone rotating in the reverse direction, through total angle $2\pi - \psi > \pi > \psi$, takes longer passage time than from A to B, through total angle ψ.

For, with fixed $\rho \geq \frac{3}{2}$ the brachistochrones are unbounded, and we have shewn that t is an increasing function of ϑ. And, with $\rho \leq \frac{3}{2}$, the speed v is bounded (1) by $v(\rho) \leq v\left(\frac{3}{2}\right) = \sqrt{2/3}$. Any path which winds once around the centre (with $r \geq 1$) has arclength at least 2π, and hence the time required is at least $2\pi/\sqrt{2/3} > 7{\cdot}6895$. For a particle winding once or more around O, which occurs close to the circle with radius $\frac{3}{2}$ (cf. Figure 5 & Figure 16), the period required for each winding is close to $3\pi/\sqrt{2/3} = 11{\cdot}54294847145677686$.

If B lies in or on the critical circle $r = \frac{3}{2}$, then the brachistochrone passage time will be maximum for B at $(\frac{3}{2}, \pi)$, and that passage time (cf. Table 1) is $6{\cdot}389577863673719$. That maximum passage time is slightly greater than $t = 6{\cdot}389572482346162$ for the Critical Brachistochrone at $\vartheta = \pi$, for which (cf. §3.1) $\tilde{r} = 1{\cdot}498409827743414$. Any path from A to B which winds around O takes a period greater than $7{\cdot}6895$.

Hence, for $\rho \leq \frac{3}{2}$, the brachistochrone AB with total angle $\psi \leq \pi$ takes less passage time than does any of the denumerable infinity of brachistochrones ending at B, which wind once or more (in either direction) around the centre. Therefore that curve is the unique curve of quickest descent from A to B — except that if $\psi = \pi$ then the plane curve can be rotated through any angle around OA.

6.2 Computation of Brachistochrones Through Two Points

In order to compute any brachistochrone AB, we need to compute the parameter J for the brachistochrone passing through the endpoint B, with radius ρ and total angle ψ (not necessarily $\leq \pi$).

The radius ρ determines some useful bounds for J, without taking the angle ψ into account. If $\rho \geq \frac{3}{2}$ then $0 \leq J < \frac{27}{4}$. If $1 < \rho < \frac{3}{2}$ and $J > \rho^3/(\rho - 1)$, then the maximum radius would be $R < \rho$, which is impossible. Therefore, if $1 < \rho < \frac{3}{2}$, then $0 \leq J \leq \rho^3/(\rho - 1)$. If $\rho = 1$ then the brachistochrone is a complete bounded brachistochrone, with $J > \frac{27}{4}$, (unless $\psi = 0$, in which case J can have any non–negative value).

For fixed radius $\rho \geq 1$, the total angle is given as a function $\Omega(J)$ of the parameter J, where (41) for unbounded brachistochrones,

$$\Omega(J) \stackrel{\text{def}}{=} \int_0^{\sqrt{\rho-1}} \frac{2\sqrt{J}\, y^2}{(1+y^2)\sqrt{(1+y^2)^3 - Jy^2}}\, \mathrm{d}y \qquad \left(J < \tfrac{27}{4}\right) . \tag{48}$$

However, for $\rho \gg 1$, $\Omega(J)$ is better computed as in (42):

$$\Omega(J) \stackrel{\text{def}}{=} \int_0^{\sqrt{1-1/\rho}} 2u^2 \sqrt{\frac{J}{1 - Ju^2(1-u^2)^2}}\, \mathrm{d}u\ , \qquad (\rho \gg 1). \tag{49}$$

For the Critical Brachistochrone (cf. (29))

$$\Omega(J) \stackrel{\text{def}}{=} \frac{1}{\sqrt{3}} \log\left(\frac{5\rho - 3 + 3\sqrt{(\rho-1)(\rho+3)}}{6 - 4\rho}\right) - 2\ \arccos\left(\frac{1}{2}\sqrt{1 + \frac{3}{\rho}}\right) \qquad \left(J = \tfrac{27}{4}\right) . \tag{50}$$

For bounded brachistochrones, compute the maximum radius R from J by Vieta's method (11), and then (19) compute

$$\zeta(\rho) \ = \ \arccos\left(\frac{2\rho - 1 - R}{1 - R}\right). \tag{51}$$

The endpoint B is on the first half–arch, if and only if ψ is less than or equal to the apsidal angle $\Theta(R, R)$ (cf. (22)). In that case (21),

$$\Omega(J) \stackrel{\text{def}}{=} \int_0^{\zeta(\rho)} \frac{x-1}{x} \sqrt{\frac{R^3}{R^2 - (R-1)x(x+R)}}\, \mathrm{d}\zeta\ , \qquad \left(J > \tfrac{27}{4},\ \psi \leq \Theta(R,R)\right)\ , \tag{52}$$

where (18),

$$x \ = \ x(\zeta) \ = \tfrac{1}{2}(1 + R - (R-1)\cos\,\zeta). \tag{53}$$

Otherwise, the endpoint is on the second half–arch, with (16),

$$\Omega(J) \stackrel{\text{def}}{=} 2\Theta(R,R) - \int_0^{\zeta(\rho)} \frac{x-1}{x} \sqrt{\frac{R^3}{R^2 - (R-1)x(x+R)}}\, \mathrm{d}\zeta\ , \qquad \left(J > \tfrac{27}{4},\ \psi > \Theta(R,R)\right)\ . \tag{54}$$

Thus, the construction of the brachistochrone AB has been reduced to computation of the unique non–negative root $J = \tilde{J}$ of the equation

$$\Omega(J) \;=\; \psi. \tag{55}$$

For any fixed $\rho \geq 1$, the function $\Omega(J)$ can be computed from (48), (49), (50), (52) and (54).

The equation (55) can readily be solved to high accuracy by the secant method, which requires evaluation of the function Ω and which requires two initial estimates J_0 and J_1. When the pair of initial estimates are such that the secant method does converge to a root ($J_n \to \tilde{J}$), then it converges (for a C^2 function) with order $\gamma = (\sqrt{5}+1)/2 = 1{\cdot}6180340$. Since the convergence is of order $\gamma > 1$ (which is faster than linear), then $(J_n - \tilde{J})/(J_n - J_{n-1}) \to 0$ as $n \to \infty$, and so the limit $\tilde{J}$ can reliably be estimated.

Once $\tilde{J}$ has been computed, then the arclength AB can be computed from (24), (30), (3) and (16); and the minimum passage time from A to B can be computed from (26), (31), (44) and (16).

If the computed root $\tilde{J}$ differs from $\frac{27}{4}$ by less than some suitable $\epsilon \ll 1$, which allows for roundoff in the arithmetic which has been performed, then the brachistochrone AB is computationally indistinguishable from an arc of the Critical Brachistochrone, with $J = \frac{27}{4}$ exactly.

6.3 Examples of Construction of Brachistochrone Through Two Points

Many examples of brachistochrones through two points have been computed by a program written in Lightspeed PASCAL, using extended variables which have roundoff corresponding to 18 or 19 significant decimal figures. Some examples are presented in Table 1, with initial estimates based on Figure 23. In each case, the secant method ended with two successive estimates of J differing by less than 10^{-16}. (Some other initial estimates J_0 & J_1 gave divergence.)

Here, ρ and ψ give the polar coordinates of the endpoint B,
J_0 and J_1 are the initial estimates given for J,
Steps is the number of steps performed of the secant method,
$\tilde{J}$ is the computed value for J,
s is the arclength of the brachistochrone AB, and
t is the time for the particle to reach the endpoint B.

6.3.1 Ill–conditioning of Brachistochrones Specified by $\rho \approx 1{\cdot}5$

The set of brachistochrones for various J, all radiating from A, diverge increasingly from each other (cf. Figure 23) as the total angle ϑ increases. Hence, extrapolation of a brachistochrone AB far beyond B is likely to be ill–conditioned, with a small perturbation of B producing large changes in the extrapolation of that brachistochrone for $\vartheta \gg \psi$.

For bounded brachistochrones, as the maximum radius $R \nearrow 1{\cdot}5$, the apsidal angle $\Theta(R,R) \nearrow \infty$. With $R = \tilde{R} = 1{\cdot}49682968195505$ the apsidal angle is π, and hence that bounded brachistochrone intersects itself at total angle $\vartheta = 2\pi \equiv 0$ (Figure 4).

Table 1

ρ	ψ	J_0	J_1	**Steps**	**Brachistochrone** AB
1·4	0·1	0·6	0·7	6	$\tilde{R} = 0{\cdot}872076056629092$ $s = 0{\cdot}419311903020327$ $t = 0{\cdot}984759549092403$
3	0·5	1·4	1·5	5	$\tilde{R} = 1{\cdot}548921707593671$ $s = 2{\cdot}200383410491580$ $t = 2{\cdot}773772083065402$
9	1	3	4	6	$\tilde{R} = 2{\cdot}456624382621970$ $s = 8{\cdot}582423395049186$ $t = 7{\cdot}837962277106861$
1·5	0·5	5·5	4	8	$\tilde{R} = 5{\cdot}207789936019642$ $s = 0{\cdot}833434497671683$ $t = 1{\cdot}589538789130731$
2	2	6·5	6·6	7	$\tilde{R} = 6{\cdot}526594013602628$ $s = 3{\cdot}247630703445667$ $t = 4{\cdot}427655052671796$
1·6	2·5	6·73	6·74	7	$\tilde{R} = 6{\cdot}731116339083094$ $s = 3{\cdot}707614023817799$ $t = 5{\cdot}218744797892048$
1·5	π	6·7498	6·7499	6	$\tilde{R} = 6{\cdot}749908390488774$ $s = 4{\cdot}606462723795077$ $t = 6{\cdot}389577863673719$
1·4	2·5	6·76	6·77	7	$\tilde{R} = 6{\cdot}766501329349459$ $s = 3{\cdot}594995649599756$ $t = 5{\cdot}217482740216487$
1	1·7	7	8	9	$\tilde{R} = 7{\cdot}025011592915404$ $s = 2{\cdot}363245968407452$ $t = 4{\cdot}338561976703014$
1·2	0·5	8	9	8	$\tilde{R} = 8{\cdot}463674646283423$ $s = 0{\cdot}657266036688363$ $t = 1{\cdot}504784387506083$
1	0·7	9	10	7	$\tilde{R} = 8{\cdot}935812016699623$ $s = 0{\cdot}933614885085511$ $t = 2{\cdot}386945822462909$

All bounded brachistochrones with apsidal angle $\Theta(R,R) < \pi$ have radius everywhere $r \leq R < \tilde{R}$, and all self–intersecting brachistochrones have maximum radius R, where $\tilde{R} \leq R < 1{\cdot}5$. With constant angle ψ, as $R \nearrow 1{\cdot}5$ and the apsidal angle $\Theta(R,R) \nearrow \infty$, the radius ρ increases asymptotically towards the radius there for the Critical Brachistochrone. At total angle $\psi = \pi$, the radius $\rho = \tilde{r} = 1{\cdot}498409827743414$ specifies the Critical Brachistochrone (cf.§3.1).

Accordingly, at angle $\psi = \pi$, those brachistochrones with apsidal angle $\Theta(R,R) < \pi$, and only those, have $1 \leq r < \tilde{R}$. At $\psi = \pi$, all of the self–intersecting brachistochrones (with unbounded apsidal angle $\Theta(R,R) \geq \pi$) have radius in the small range

$$1{\cdot}49682968195505 \;=\; \tilde{R} \;\leq r \;<\; \tilde{r} \;=\; 1{\cdot}498409827743414 \;.$$

Thus, for brachistochrones specified by the endpoint $B = (\rho, \pi)$, as ρ increases from $\tilde{R} = 1{\cdot}49682968195505$ towards $\tilde{r} = 1{\cdot}498409827743414$, the complete brachistochrones are all self–intersecting, with total angle increasing from 2π — unboundedly. Hence, the computation of complete brachistochrones is inherently ill–conditioned, when extrapolated from endpoints in that small range.

A small perturbation of B, crossing the Critical Brachistochrone from $J > 6{\cdot}75$ to $J < 6{\cdot}75$, would change the nature of the solution from a bounded to an unbounded brachistochrone. And for unbounded brachistochrones, small perturbations of the endpoint with ρ close to $1{\cdot}5$ can produce much larger changes in the asymptotic angle (cf. Figure 23).

However, in all such cases the arc AB may be computed to high accuracy, even though the behaviour of the brachistochrone extrapolated far beyond B might be markedly altered by a small perturbation of B. For example, with $\rho < 1{\cdot}5$, if ψ is sufficiently close to $\vartheta(\rho)$ as given by (29), then the arc of the Critical Brachistochrone from $r = 1$ to $r = \rho$ is a good approximation to the brachistochrone AB.

Acknowledgments

I wish to thank Ron Keam and Don Nield, for stimulating discussions about this problem.

References

1. Tee, G. J. (1999), Isochrones and brachistochrones. *Dynamic Systems and Applications*, (to appear).

1999–2–15